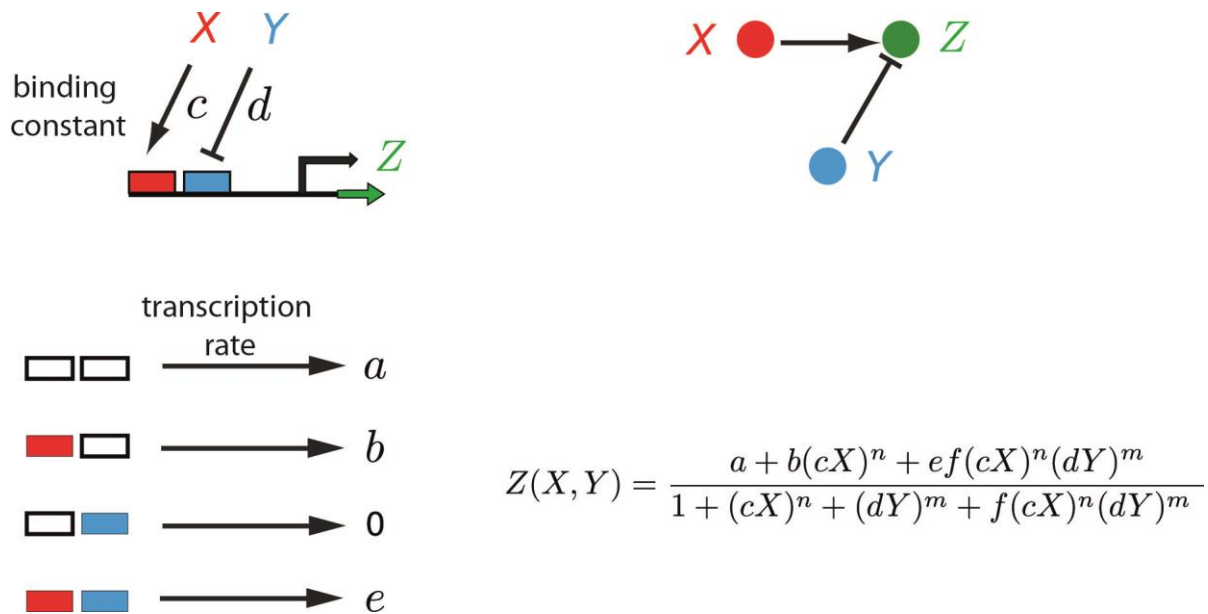
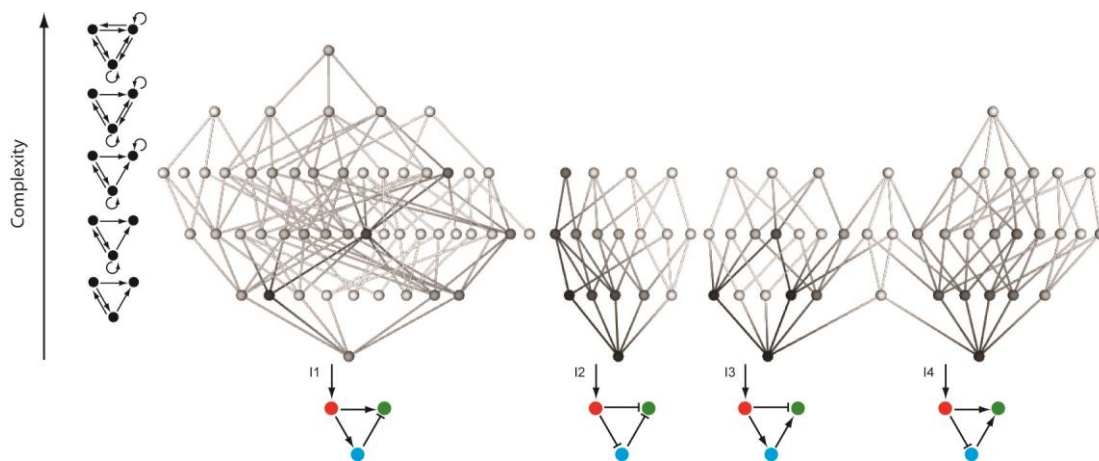


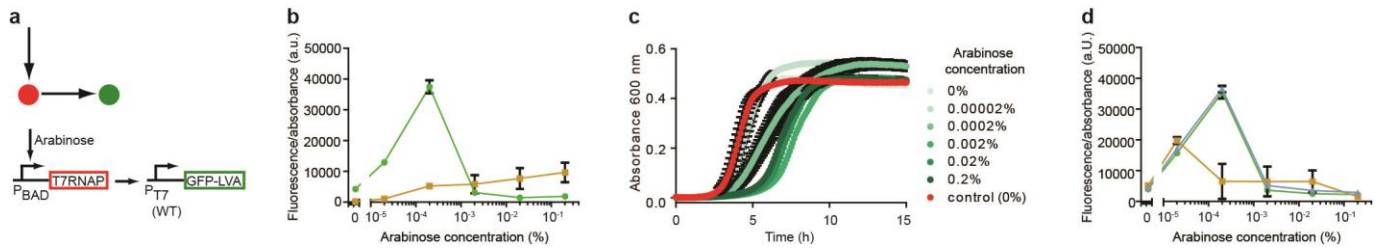
Supplementary Figures



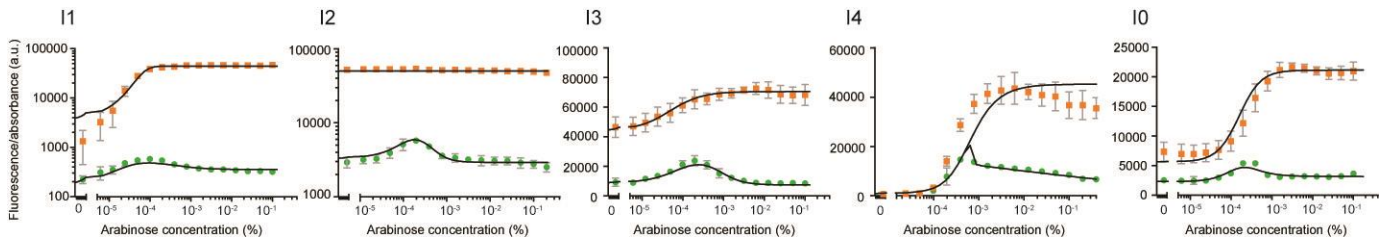
Supplementary Figure 1. The model. The definition of the employed function with a , b and e being related to the transcriptional rates from the free promoter, from the promoter bound with one factor, and from the promoter bound with both factors, respectively; c and d being the binding constants of the two factors X and Y , respectively; f , the binding cooperativity/competition constant of the binding of X and Y ; and n and m being the multimerization or cooperativity coefficients (i.e. generally referred to as Hill coefficients). See also the associated Supplementary Table 1.



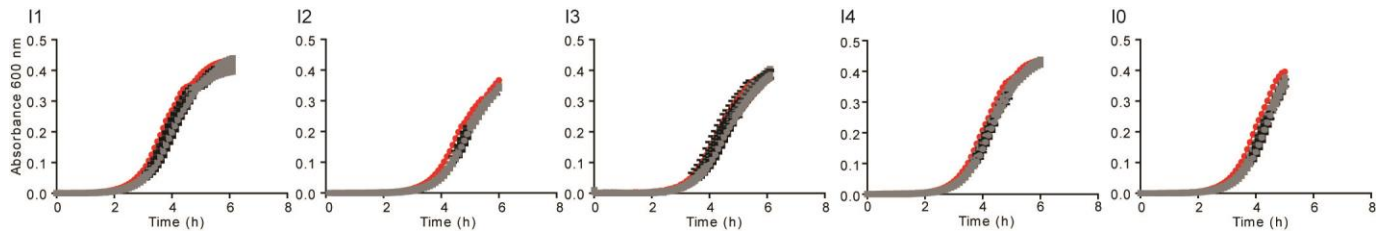
Supplementary Figure 2. Mutational robustness of the networks. Mutational robustness, as measured by the fraction of functional parameter space, is shown by the shading (darker topologies are more robust).



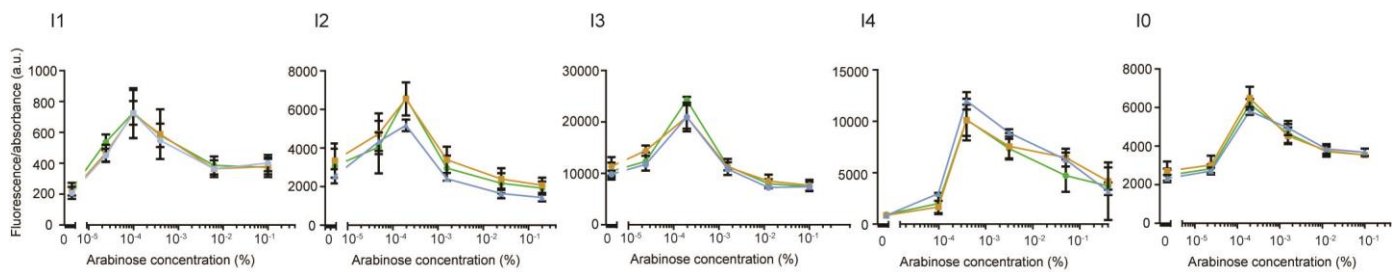
Supplementary Figure 3. Example of a network causing metabolic load. (a), The tested network topology is a relay and the expectation is that increasing input (arabinose) should simply lead to increasing output (GFP-LVA). (b), Unexpected stripe behavior in the tested network (green). The same network topology can behave as originally expected (orange) if the expression levels are lowered so as not to cause metabolic stress in the cells. In this case, load was reduced by tagging the T7 RNAP with an UmuD degradation tag, using a mutant T7 promoter and inserting a sequence with a strong secondary structure after the promoter. (c), The network with metabolic load causes increased lag phases and slower growth rates at high arabinose concentrations compared to control cells (red). (d), A re-growth experiment: Cells were grown and assayed for 15 h. The cells grown at 0% arabinose and at 0.2% were diluted into fresh medium, re-grown to stationary phase and together with freshly picked cells from the original agar plate again assayed at 6 arabinose concentrations. The cells previously grown at high arabinose concentration (orange) show a different behavior to cells previously grown at 0% arabinose (green) or freshly picked cells from the agar plate (blue), indicating that this network also fails our engineering criteria (Fig. 3) at this level.



Supplementary Figure 4. Metabolic load controls with increased expression mutants. WT and mutant networks are shown in green and orange, respectively (c.f. Fig. 5, bottom row and Supplementary Fig. 7). The mutants are identical to the WT networks except that repressor activities were reduced by adding IPTG (I1, I2, I3) or aTc (I4, I5). This leads to increased expression of the network output (GFP). As these mutants do not display an unexpected stripe phenotype (c.f. Supplementary Fig. 3) they demonstrate that the WT networks are not at the metabolic load limit. For the fluorescence/absorbance data, the mean and the standard deviation from 3 biological replicates are shown.



Supplementary Figure 5. Growth curves of network constructs (metabolic load controls). A characteristic of metabolic load is long lag times at high inducer concentrations (Supplementary Fig. 3). Therefore all networks built in this study were tested for potential growth lags with arabinose induction. The absorbance (600 nm) was recorded for bacteria containing the indicated WT network, grown at 16 different concentrations of arabinose (between 0 and 0.4%, all grey) and of control cells (red) transformed with the empty plasmids at 0% arabinose. The mean and the standard deviation from 3 biological replicates are shown. As seen above, the final network topologies built in this study do not display severe lag times with varying arabinose.

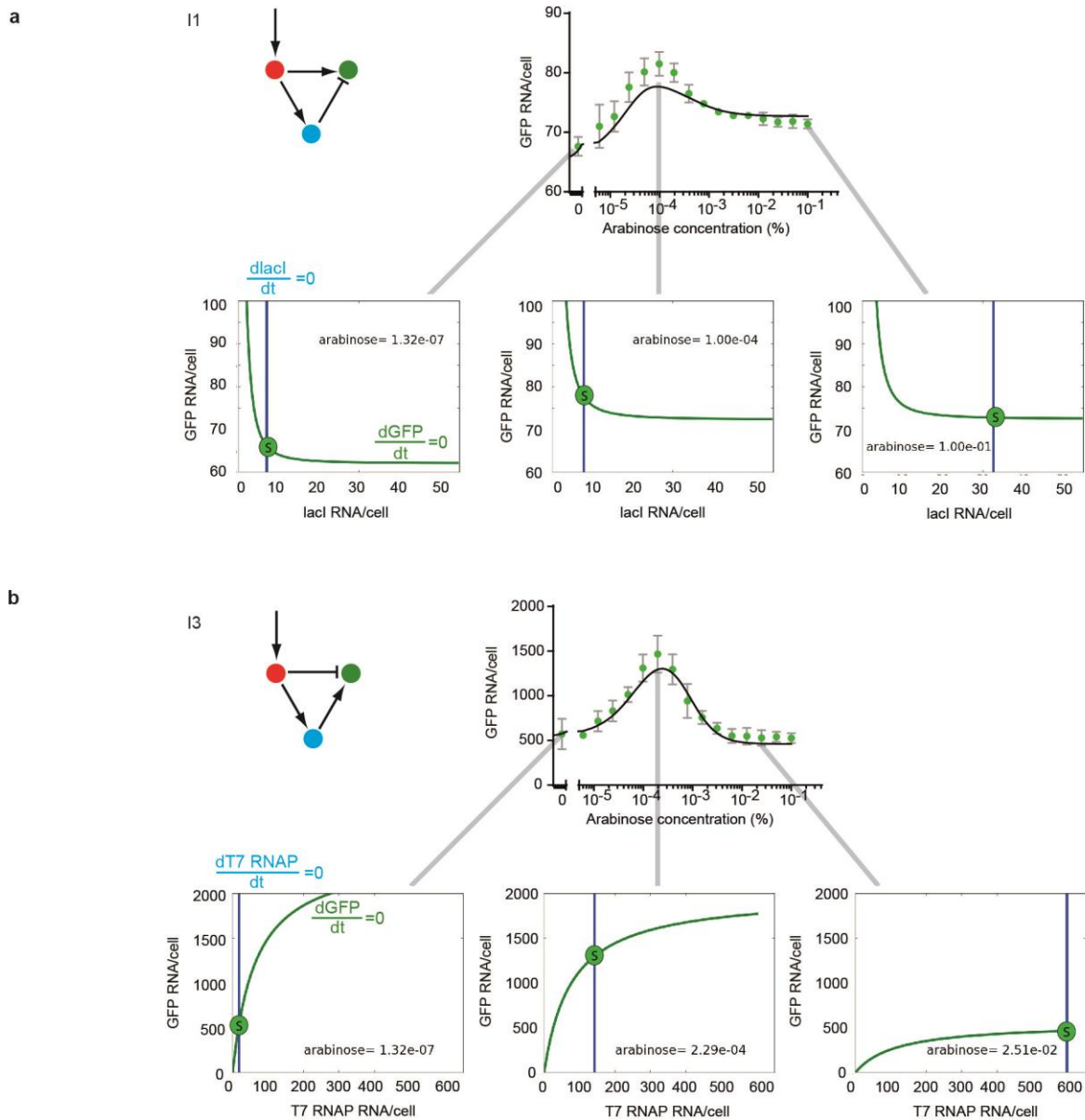


Supplementary Figure 6. Re-growth controls for the exclusion of inactivating mutations. Cells containing the indicated WT network were picked from an agar plate, grown and assayed (Fig. 4). The cells grown at 0% arabinose (green) and at the highest arabinose concentration (0.1, 0.2 or 0.4%, orange) were diluted into fresh medium, grown overnight and together with freshly picked cells from the original agar plate (blue) again assayed at 6 arabinose concentrations. The mean and the standard deviation from 3 biological replicates are shown. The samples all regenerate stripes and are therefore 'true breeding', implying that inactivating mutations¹ are not responsible for the low GFP expression at high arabinose concentrations.

	WT network	mutant 1	mutant 2	mutant 3
I1		<p>P_{SP6}(WT) → P_{SP6}(-16G)</p> <p>- SP6 RNAP binding decreased</p>	<p>P_{SP6}(-11C) → P_{SP6}(-2G,-11C)</p> <p>- SP6 RNAP transcription initiation decreased</p>	<p>+ 300 μM IPTG</p> <p>- concentration of active lacI decreased</p>
I2		<p>J23114 → J23109</p> <p>+ 5 μM IPTG</p> <p>- weaker constitutive promoter</p>	<p>+ 0.005 μM aTc + 5 μM IPTG</p> <p>- concentration of active TetR decreased</p>	<p>+ 700 μM IPTG</p> <p>- concentration of active lacI decreased</p>
I3		<p>P_{SP6}(-13T) → P_{SP6}(-6T)</p> <p>- SP6 RNAP binding increased</p>	<p>P_{T7}(-3G) → P_{T7}(-14G)</p> <p>- T7 RNAP binding decreased, transcription initiation changed</p>	<p>+ 100 μM IPTG</p> <p>- concentration of active lacI decreased</p>
I4		<p>P_{T7}(-14G) → P_{T7}(-5T)</p> <p>- T7 RNAP binding decreased</p>	<p>J23106 → J23105</p> <p>- weaker constitutive promoter</p>	<p>+ 0.1 μM aTc</p> <p>- concentration of active TetR decreased</p>
I0		<p>antistripe 1 + 0 μM aTc</p> <p>- concentration of active TetR increased</p>	<p>antistripe 2 + 0.2 μM aTc</p> <p>- concentration of active TetR decreased</p>	
		<p>P_{SP6}(-6T) → P_{SP6}(-16G) + 0.125 μM aTc</p> <p>- SP6 RNAP binding increased</p>	<p>antistripe 4 P_{SP6}(-6T) → P_{SP6}(-16G) + 0 μM aTc</p> <p>- SP6 RNAP binding increased, concentration of active TetR decreased</p>	
		<p>P_{SP6}(-6T) → P_{SP6}(-16G) + 0.2 μM aTc</p> <p>- SP6 RNAP binding increased, concentration of active TetR decreased</p>	<p>antistripe 5 P_{SP6}(-6T) → P_{SP6}(-16G) + 0.2 μM aTc</p> <p>- SP6 RNAP binding increased, concentration of active TetR decreased</p>	

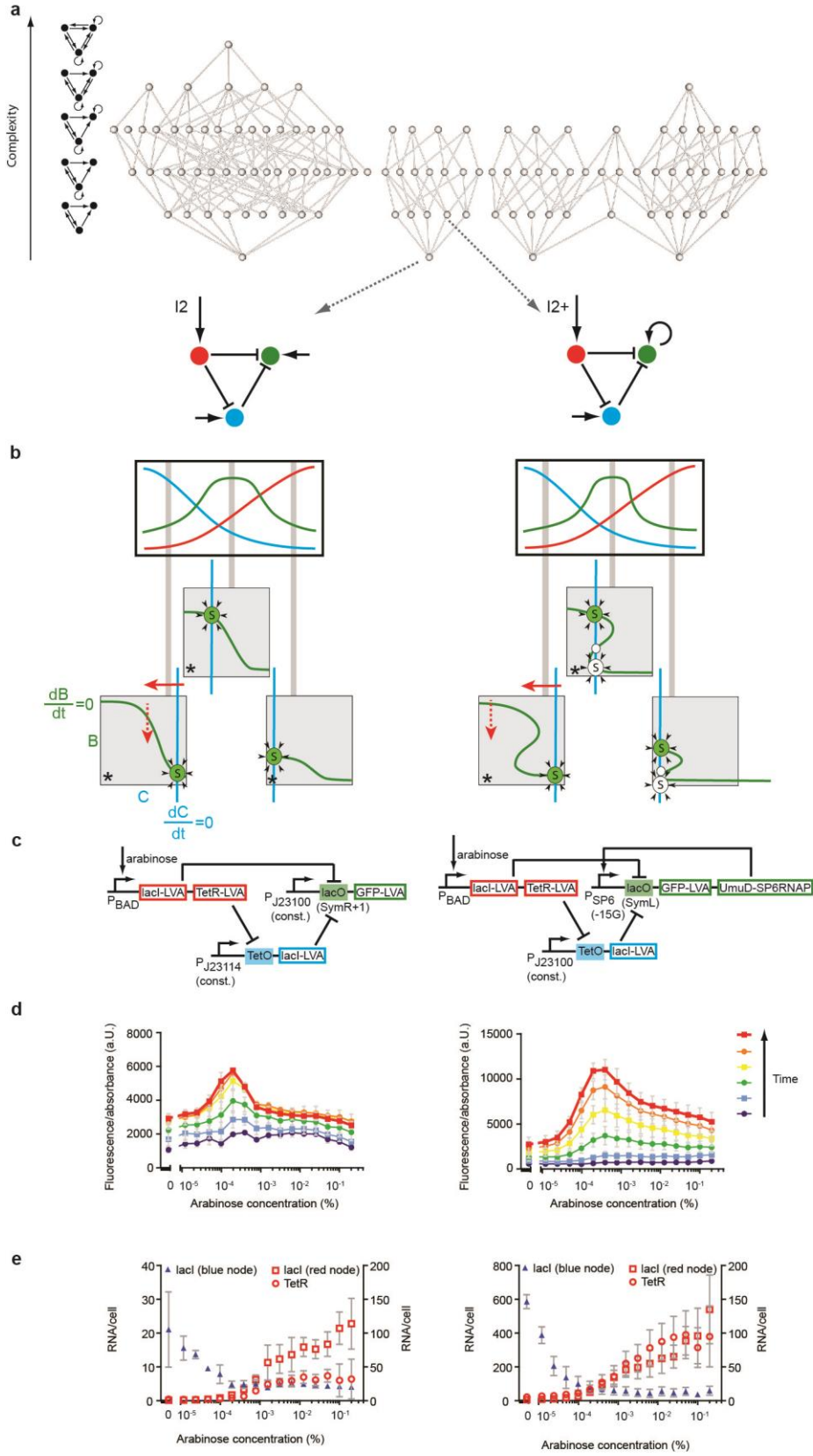
Supplementary Figure 7. I1, I2, I3, I4, I0 networks and related mutants. The first column depicts the network implementations and conditions for the wild-type (WT) networks. Unshaded and shaded boxes represent genes and repressor binding sites, respectively. The next three to five columns describe the changes for the mutants shown in Fig. 5 (I1-I4), Fig. 6 and Supplementary Fig. 10 (I0). The changed interactions are highlighted (asterisk, orange) in the topologies. Abbreviations: P_{BAD}: arabinose-responsive promoter; GFP: superfolder green fluorescent protein²; LVA: degradation signal³; UmuD: degradation signal⁴; SP6 RNAP or T7 RNAP: SP6 or T7 phage RNA polymerase; T7 RNAP N or T7 RNAP C: N- or C-terminal fragment of

split T7 RNAP⁵. P_{SP6} or P_{T7}: SP6 or T7 promoter; promoter mutants are shown in brackets, numbered relative to the transcription start site e.g. (-11C); lacI: lactose operon repressor protein; lacO: lac operator (SymR+1, SymL: mutants⁶); IPTG: isopropyl β-D-1-thiogalactopyranoside; TetR: tetracycline repressor; TetO: Tet operator; aTc: anhydrotetracycline; P_{J23100}, P_{J23105}, P_{J23106}, P_{J23114} and P_{J23109}: constitutive (const.) promoters (<http://partsregistry.org/Promoters/Catalog/Anderson>).

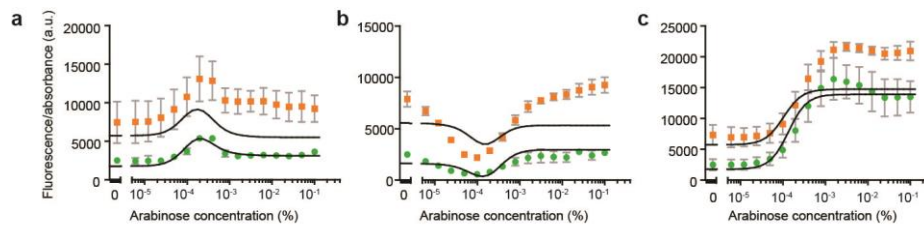


Supplementary Figure 8. Nullclines from experimental data. (a) Nullclines of I1. The parameters used for this graphs are included in Supplementary Table 3. We plot the formula of GFP_{WT} from Supplementary Table 3 as a function of the inhibitor concentration (gene C, lacI). The formation of the stripe occurs through the movement of the blue nullcline (gene C, lacI) rightwards, and through the reduction of the green sigmoidal nullcline downwards. **(b)** Nullclines of I3. The parameters used for this graphs are included in

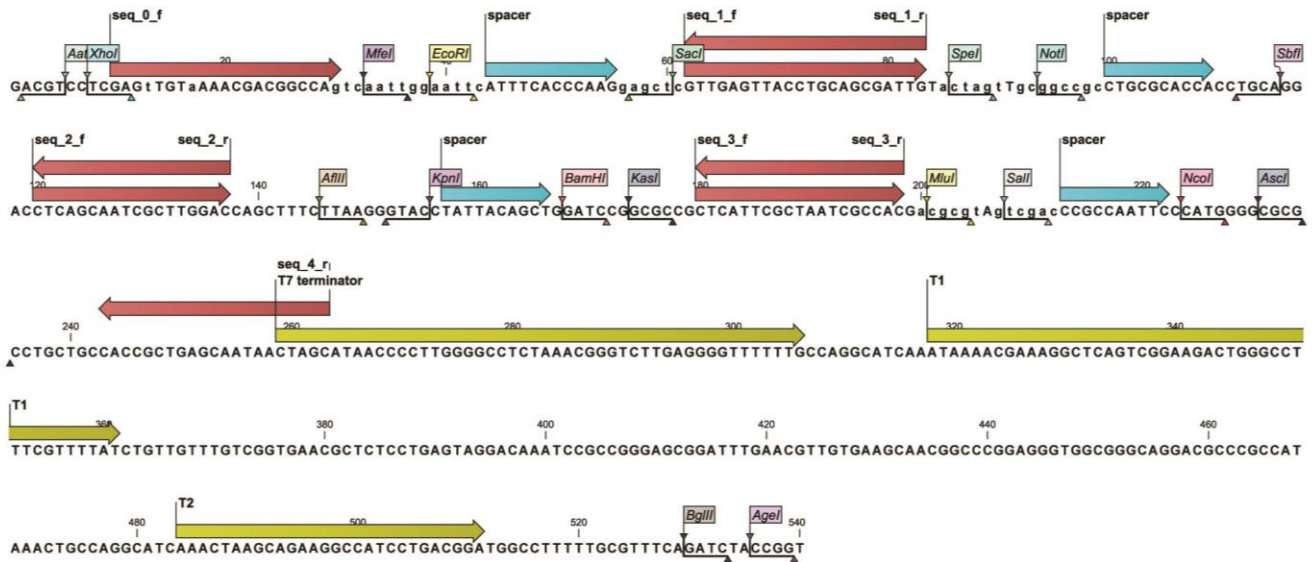
Supplementary Table 5. We plot the formula of GFP_{WT} from Supplementary Table 5 as a function of the activator concentration (gene C, T7 RNAP). Note that the curve is of Michaelis-Menten type, as $n=1$. The formation of the stripe occurs through the movement of the blue nullcline (gene C, T7 RNAP) rightwards, and through the reduction of the green sigmoidal nullcline downwards.



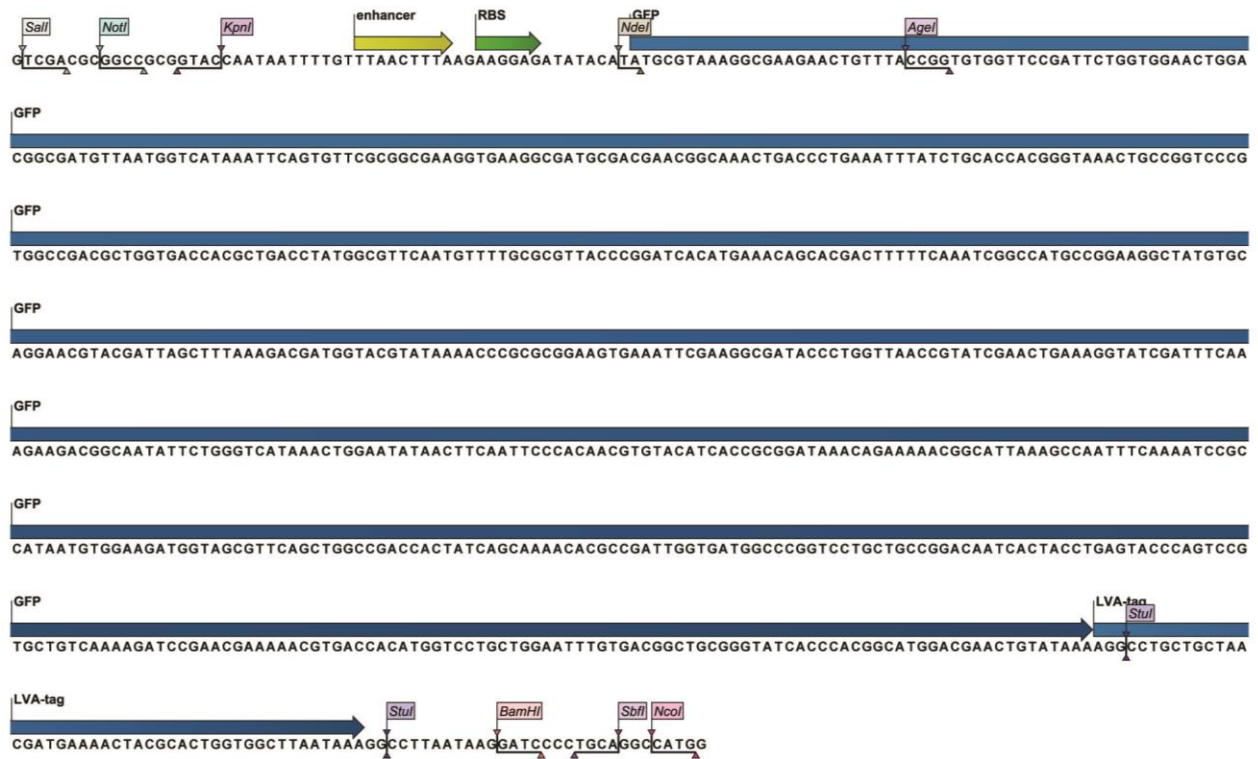
Supplementary Figure 9: Networks within the same stalactite have the same mechanism. (a), Two networks of the I2 stalactite were built: The minimal network (I2, left, Fig. 1, 4-5) and a network with a self-activation, as opposed to constitutive activation, on the green node (I2+, right). Their positions in the complexity atlas are indicated with an arrow. (b), Phase portraits for the two networks at low, medium and high morphogen concentration were calculated from examples from the atlas (with the following parameters: $AB = -10.72$; $AC = -2.0$; $CB = -8$; and the self-activation $BB = 2.0$). The x-axis represents the activity of the blue gene (i.e. C) and the y-axis, the activity of the green gene (i.e. B). The nullcline curves (where one variable does not change in time) of the blue and green genes are shown as colored lines. Where they intersect are the stable steady states (S) or the unstable steady states (small white circles). The black star indicates the initial condition close to the origin. The full red arrows in these phase plots show that the nullclines move only horizontally in response to the morphogen gradient and the dashed red arrows indicate the decrease in the height of the nullcline. Although the I2+ network shows bistability, it is clear that it can be generated by a smooth transform of the I2 network: the positive feedback causing the green nullcline to fold back on itself. (c), Implementations of the circuits in the network scaffold. (d), *E. coli* transformed with each network display single fluorescent stripes in arabinose gradients as measured by fluorescence spectrometry (normalized by the absorbance). Time course: 12 min intervals, at 5 - 6 h of growth. Mean and s.d. from 3 biological replicates. (e), Measured mRNA concentrations for all genes other than the stripe-forming gene. Mean and s.d. from 3 biological replicates.



Supplementary Figure 10. Predictions for additional mutants of the 2-node archetype network (I0). The model was simultaneously fitted (black lines, Supplementary Table 2) to the mRNA data, the WT network (a, green) and mutant 1 (b, green) and mutant 2 (c, green). Mutant 3 (a, orange), mutant 4 (b, orange) and mutant 5 (c, orange) differ from these networks by the utilized variant of the SP6 promoter. The constructs in orange employ the promoter $P_{SP6(-16G)}$ that has a 2.5-fold higher activity than the promoter of the constructs in green ($P_{SP6(-6T)}$)⁷. We therefore inserted this factor of 2.5 into our model obtained from fitting the green constructs, to predict the behavior of the mutants 3-5. A good agreement between the predictions (black lines) and the measured fluorescence data (orange) was thus obtained. The mean and the standard deviation from 3 biological replicates are shown. The exact changes and conditions are listed in Supplementary Fig. 7.

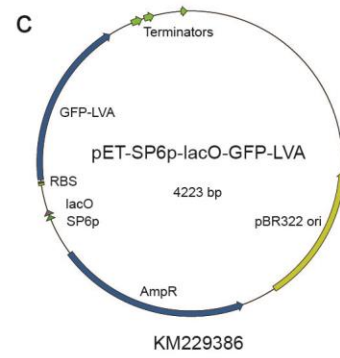
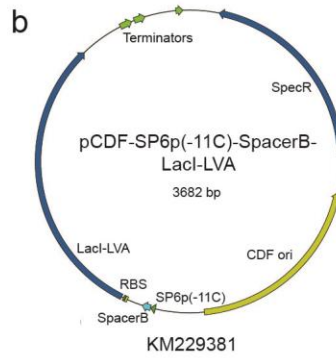
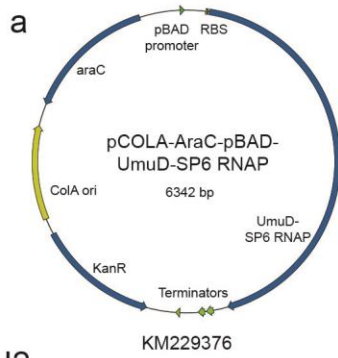


Supplementary Figure 11. Design of the multiple cloning site (MCS). Promoters and repressor binding sites are cloned between EcoRI and SacI. Three spacers occupy the place where genes and their ribosomal binding sites (RBS) can be cloned. These are found between (1) NotI and SbfI, (2) KpnI and BamHI, and (3) SalI and NcoI. Pairs of alternative restriction sites also flank each gene insertion site: (1) SpeI and BbvCI, (2) Afl II and KasI, and (3) MluI and AscI. Primers (labeled “seq”) are used for verifying gene insertion and for sequencing. Multiple transcription terminators (T7 terminator, rrnB terminators T1 and T2) compose the end of the MCS.

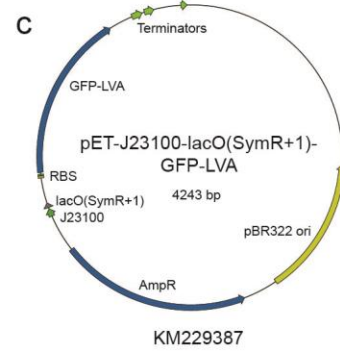
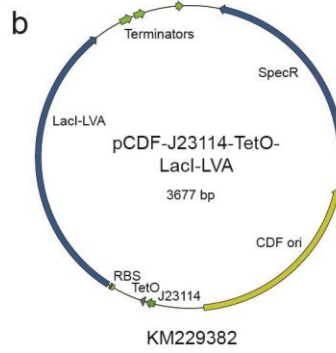
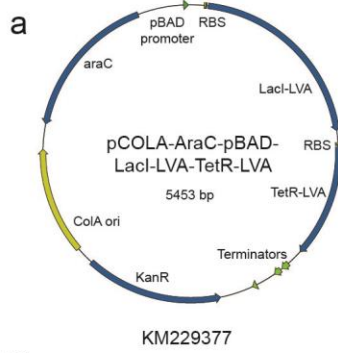


Supplementary Figure 12. Generic sequences flanking the genes in pUC57. The gene coding for superfolder GFP with the LVA degradation tag is shown as an example.

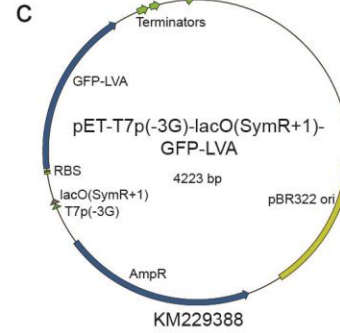
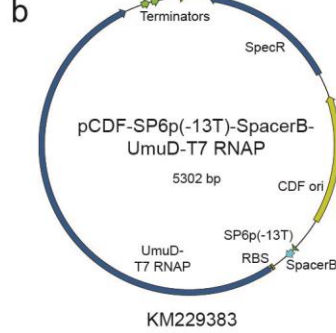
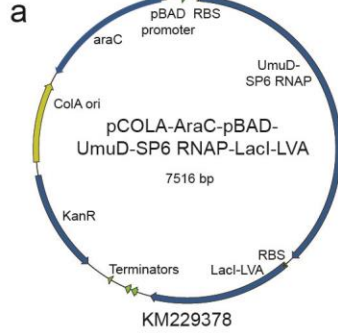
I1



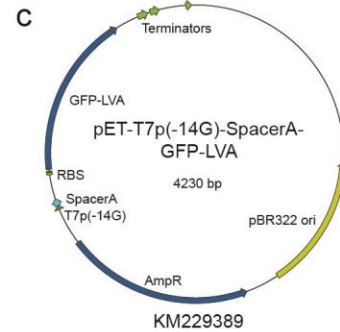
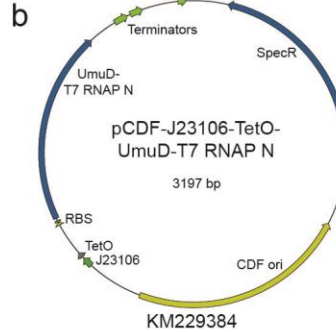
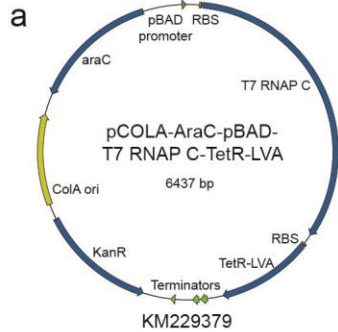
I2

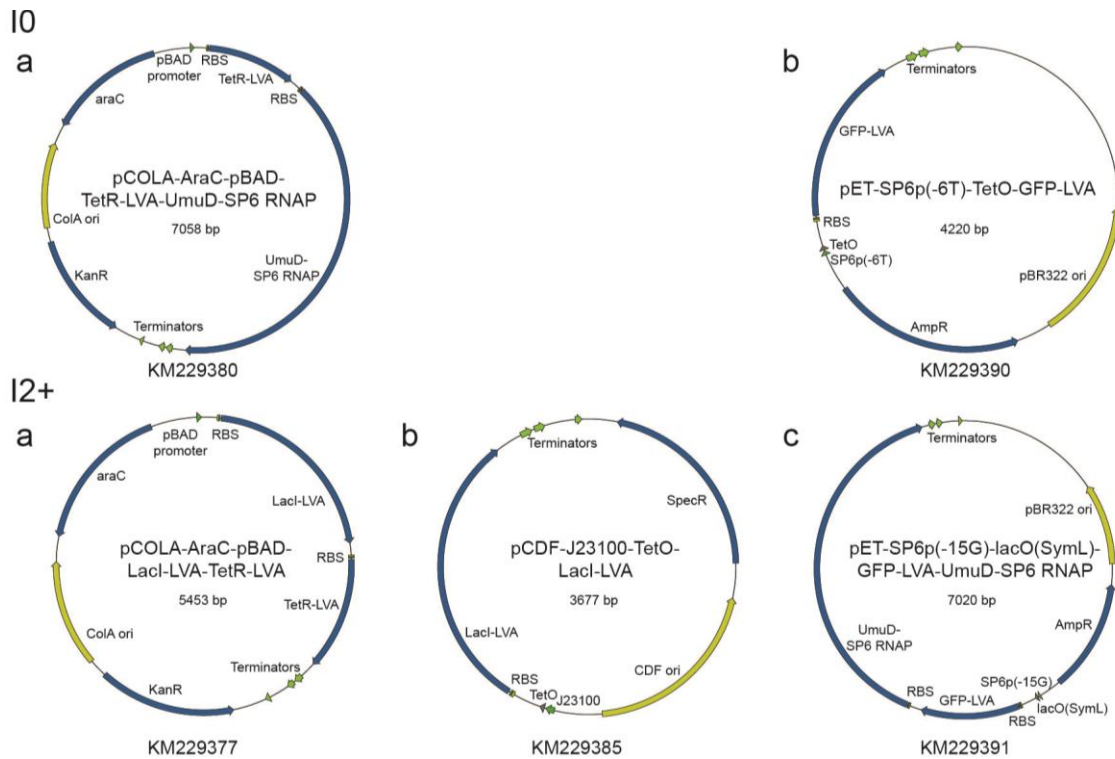


I3

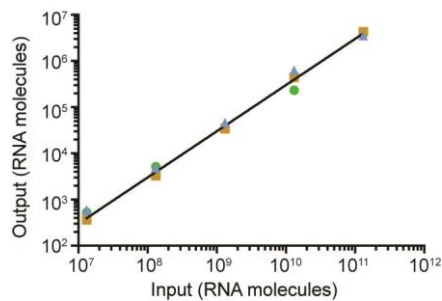


I4





Supplementary Figure 13. Plasmid maps for the networks built in this study. The 3-node networks, were built with one node on each of the 3 compatible plasmids (pCOLA, pCDF, pET). The 2-node archetypal stripe-forming (I0) network was built with 2 plasmids (pCOLA, pET). The GenBank accession codes are given at the bottom of each plasmid.

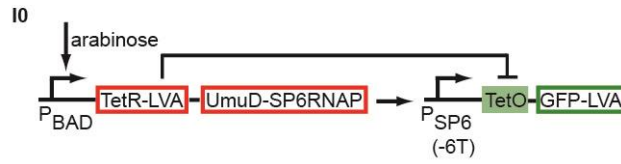


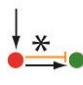
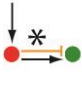
Supplementary Figure 14. The recovery of the spike RNA is linear and constant. Different amounts of spike RNA were added to cell samples with low (green circles), medium (orange squares) and high expression (blue triangles) of a synthetic network. The RNA of the samples was extracted and reverse transcribed and quantified by qPCR. The amount of measured output spike molecules was proportional to the amount added to each sample and independent of the network expression level. For subsequent experiments, 2 ng (1.31×10^9 molecules) of spike RNA were added to each sample. Thus, the absolute RNA production of each network node per cell could be estimated (see Supplementary Methods).

Supplementary Tables

Parameter	Definition	Mutations might affect
a	$\alpha \frac{N_{GFP}}{\delta_{mGFP}} Q$	α
b	$\beta \frac{N_{GFP}}{\delta_{mGFP}} Q$	β
c	$K_x \frac{k_{tl,X}}{\delta_s Q}$	K_x
d	$\frac{k_{tl,X}}{\delta_T Q} (K_Y k_m)^{1/m}$	K_Y
e	$\varepsilon \frac{N_{GFP}}{\delta_{mGFP}} Q$	ε
f	Non-dimensional factor	
n	Hill exponent	
m	Hill exponent	

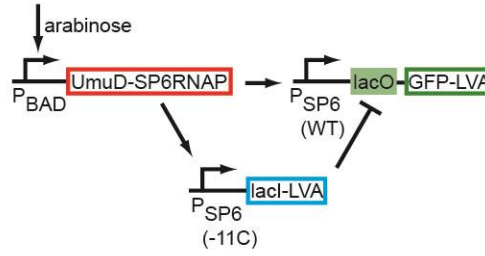
Supplementary Table 1. Definitions of the parameters. For IO as example. The notations are: α , β , ε transcription rates (nM s^{-1}); N_{GFP} , plasmid copy number; δ_{mGFP} , degradation rate of the GFP mRNA (s^{-1}); $k_{tl,S}$, $k_{tl,T}$, translation rates for the SP6 RNAP and TetR mRNAs (s^{-1}); δ_s , δ_T , degradation rates of the SP6 RNAP and TetR proteins (s^{-1}); k_m , multimerization constant for TetR (nM^{-1}); K_S , K_T , binding constants for SP6 RNAP and TetR (nM^{-1}); ω , non-dimensional factor including binding independence/cooperativity. Q is a re-scaling factor which allows us to convert our measurements (mRNA molecules/cell) to concentrations for the model (here $Q = 1$, i.e. 1 nM implies 1 molecule/cell¹⁶).

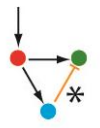
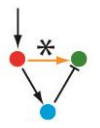
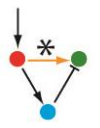
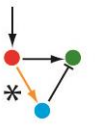


Name	Value	Constraints	Definition
a_s b_s c_s n_s	4.19e+00 1.33e+02 2.44e+03 2.02E+00		$SP6 = \frac{a_s + b_s(c_s ara)^{n_s}}{1 + (c_s ara)^{n_s}}$
a_T b_T c_T n_T	1.78e+00 5.67e+02 6.26e+02 1.24e+00		$TetR = \frac{a_T + b_T(c_T ara)^{n_T}}{1 + (c_T ara)^{n_T}}$
a b c n	0 1.65e+03 9.04e-02 1	Fixed Fixed	$GFP_{mut2} = \frac{a + b(c SP6)^n}{1 + (c SP6)^n}$ 
a b c d e f n m	0 1.65e+03 9.04e-02 3.56e-02 1.02e+03 0.1 1 2	Fixed Fixed Fixed	$GFP_{WT} = \frac{a + b(c SP6)^n + ef(c SP6)^n(d TetR)^m}{1 + (c SP6)^n + (d TetR)^m + f(c SP6)^n(d TetR)^m}$
β_T	2.83e+00		$GFP_{mut1} = \frac{a + b(c SP6)^n + ef(c SP6)^n(\beta_T d TetR)^m}{1 + (c SP6)^n + (\beta_T d TetR)^m + f(c SP6)^n(\beta_T d TetR)^m}$ 

Supplementary Table 2. Fitting of I0. The interactions marked (orange, asterisk) are modified in the mutant networks. The exact changes and conditions are listed in Supplementary Fig. 7. For mutant 2 (+ 0.2 μ M aTc) it was assumed that TetR no longer has any observable effect.

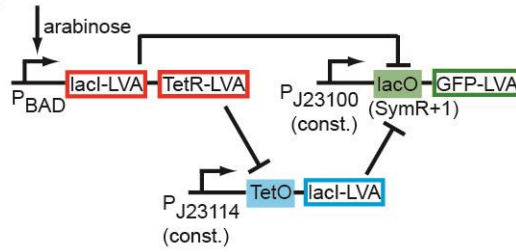
I1



Name	Value	Constraints	Definition
a_s b_s c_s n_s	8.62e-01 2.97e+01 1.11e+02 1	Fixed	$SP6 = \frac{a_s + b_s(c_s ara)^{n_s}}{1 + (c_s ara)^{n_s}}$
a_l b_l c_l n_l	4.76e+00 4.85e+01 6.45e-02 1	Fixed	$lacI = \frac{a_l + b_l(c_l ara)^{n_l}}{1 + (c_l ara)^{n_l}}$
a b c n	0 1.78e+03 1.00e+00 1.43e+01	Fixed	$GFP_{mut3} = \frac{a + b(c SP6)^n}{1 + (c SP6)^n}$ 
a b c d e f n m	0 1.78e+03 1.00e+00 3.33e-01 7.24e+01 4.65e+01 1.43e+01 2	Fixed	$GFP_{WT} = \frac{a + b(c SP6)^n + ef(c SP6)^n(d lacI)^m}{1 + (c SP6)^n + (d lacI)^m + f(c SP6)^n(d lacI)^m}$ 
α_G β_G	9.46e-01 1.00e+00		$GFP_{mut1} = \frac{a + \alpha_G b(\beta_G c SP6)^n + \alpha_G ef(\beta_G c SP6)^n(d lacI)^m}{1 + (\beta_G c SP6)^n + (d lacI)^m + f(\beta_G c SP6)^n(d lacI)^m}$ 
α_l β_l	5.00e-02 1	Fixed	$lacI_{mut2} = \frac{a_l + \alpha_l b_l(\beta_l c_l SP6)^{n_l}}{1 + (\beta_l c_l SP6)^{n_l}}$ $GFP_{mut2} = \frac{a + b(c SP6)^n + ef(c SP6)^n(d lacI_{mut2})^m}{1 + (c SP6)^n + (d lacI_{mut2})^m + f(c SP6)^n(d lacI_{mut2})^m}$ 

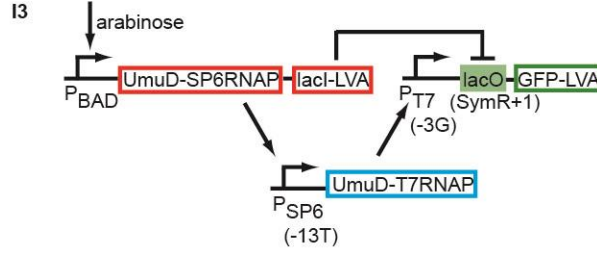
Supplementary Table 3. Fitting of I1. The interactions marked (orange, asterisk) are modified in the mutant networks. The exact changes and conditions are listed in Supplementary Fig. 7. For mutant 3 (+ 300 μ M IPTG) it was assumed that lacI no longer has any observable effect.

I2



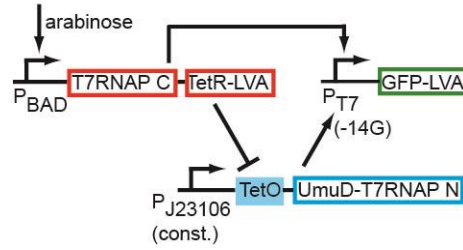
Name	Value	Constraints	Definition
a_T b_T c_T n_T	1.87e+00 4.31e+01 3.88e+02 1	Fixed	$TetR = \frac{a_T + b_T (c_T ara)^{n_T}}{1 + (c_T ara)^{n_T}}$
a_l b_l c_l n_l	5.16e-01 1.08e+02 1.30e+02 1	Fixed	$lacI_{inc} = \frac{a_l + b_l (c_l ara)^{n_l}}{1 + (c_l ara)^{n_l}}$
a_D b_D c_D n_D	1.24e+04 3.98e+00 1.65e+01 2	Fixed	$lacI_{dec} = \frac{a_D + b_D (c_D TetR)^{n_D}}{1 + (c_D TetR)^{n_D}}$
a b c n	4.40e+02 8.47e+01 2.52e-01 3.22e+00		$lacI = lacI_{inc} + lacI_{dec}$ $GFP_{WT} = \frac{a + b (c lacI)^n}{1 + (c lacI)^n}$
α	1.15e-01		$lacI_{dec,mut1} = \frac{\alpha a_D + b_D (c_D TetR)^{n_D}}{1 + (c_D TetR)^{n_D}}$ $lacI_{mut1} = lacI_{inc} + lacI_{dec,mut1}$ $GFP_{mut1} = \frac{a + b (c lacI_{mut1})^n}{1 + (c lacI_{mut1})^n}$
β	4.13e-01		$lacI_{dec,mut2} = \frac{a_D + b_D (\beta c_D TetR)^{n_D}}{1 + (\beta c_D TetR)^{n_D}}$ $lacI_{mut2} = lacI_{inc} + lacI_{dec,mut2}$ $GFP_{mut2} = \frac{a + b (c lacI_{mut2})^n}{1 + (c lacI_{mut2})^n}$
γ	6.49e-04		$GFP_{mut3} = \frac{a + b (\gamma c lacI)^n}{1 + (\gamma c lacI)^n}$

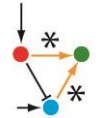
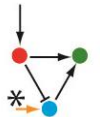
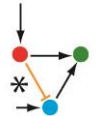
Supplementary Table 4. Fitting of I2. The interactions marked (orange, asterisk) are modified in the mutant networks. The exact changes and conditions are listed in Supplementary Fig. 7.



Name	Value	Constraints	Definition	
a_l b_l c_l n_l	2.62e+01 4.86e+02 5.88e+01 1	Fixed	$lacI = \frac{a_l + b_l(c_l ara)^{n_l}}{1 + (c_l ara)^{n_l}}$	
a_s b_s c_s n_s	7.02e+00 3.80e+02 8.45e+02 1.1		$SP6 = \frac{a_s + b_s(c_s ara)^{n_s}}{1 + (c_s ara)^{n_s}}$	
a_T b_T c_T n_T	0 1.55e+03 1.71e-03 1	Fixed Fixed	$T7 = \frac{a_T + b_T(c_T SP6)^{n_T}}{1 + (c_T SP6)^{n_T}}$	
a b c n	0 4.43+03 8.76e-02 1	Fixed Fixed	$GFP_{mut3} = \frac{a + b(c T7)^n}{1 + (c T7)^n}$	
a b c d e f n m	0 4.43e+03 8.76e-02 1.03e-01 5.42e+02 9.84e-02 1 2.35	Fixed Fixed	$GFP_{WT} = \frac{a + b(c T7)^n + ef(c T7)^n(d lacI)^m}{1 + (c T7)^n + (d lacI)^m + f(c T7)^n(d lacI)^m}$	
α_G β_G	6.33e-01 2.64e-01		$GFP_{mut2} = \frac{a + \alpha_G b(\beta_G c T7)^n + \alpha_G ef(\beta_G c T7)^n(d lacI)^m}{1 + (\beta_G c T7)^n + (d lacI)^m + f(\beta_G c T7)^n(d lacI)^m}$	
α_T β_T	1 2.04e+00	Fixed	$T7_{mut1} = \frac{a_T + \alpha_T b_T(\beta_T c_T SP6)^{n_T}}{1 + (\beta_T c_T SP6)^{n_T}}$ $GFP_{mut1} = \frac{a + b(c T7_{mut1})^n + ef(c T7_{mut1})^n(d lacI)^m}{1 + (c T7_{mut1})^n + (d lacI)^m + f(c T7_{mut1})^n(d lacI)^m}$	

Supplementary Table 5. Fitting of I3. The interactions marked (orange, asterisk) are modified in the mutant networks. The exact changes and conditions are listed in Supplementary Fig. 7. For mutant 3 (+ 100 μ M IPTG) it was assumed that lacI no longer has any observable effect.



Name	Value	Constraints	Definition
a_s b_s c_s n_s	4.88e+00 3.21e+01 1.39e+03 1.14		$T7C = \frac{a_c + b_c(c_c ara)^{n_c}}{1 + (c_c ara)^{n_c}}$
a_N b_N c_N n_N r	6.27e+02 1.29e+01 2.54e+03 1.05e+01 -4.86e-01		$T7N = \frac{a_N + [b_N + r(\log(ara) + 7)](c_N ara)^{n_N}}{1 + (c_N ara)^{n_N}}$ $T7 := \min(T7C, T7N)^2$
a b c n	0 6.25e+02 3.33e-03 1	Fixed Fixed	$GFP_{WT} = \frac{a + b(c T7)^n}{1 + (c T7)^n}$
γ	4.14e-01		$GFP_{mut1} = \frac{a + b(\gamma c T7)^n}{1 + (\gamma c T7)^n}$ 
α_N β_N	8.26e-03 8.27e-01		$T7N_{mut2} = \frac{\alpha_N a_N + [\beta_N b_N + r(\log(ara) + 7)](c_N ara)^{n_N}}{1 + (c_N ara)^{n_N}}$ $T7_{mut2} := \min(T7C, T7N_{mut2})^2$ $GFP_{mut2} = \frac{a + b(c T7_{mut2})^n}{1 + (c T7_{mut2})^n}$ 
			$T7N_{mut3} = a_N$ $T7_{mut3} := \min(T7C, T7N_{mut3})^2$ $GFP_{mut3} = \frac{a + b(c T7_{mut3})^n}{1 + (c T7_{mut3})^n}$ 

Supplementary Table 6. Fitting of I4. The interactions marked (orange, asterisk) are modified in the mutant networks. The exact changes and conditions are listed in Supplementary Fig. 7. For mutant 3 (+ 0.1 μ M aTc) it was assumed that TetR no longer has any observable effect. Due to detection problems of low concentrations of T7 RNAP N (T7N) mRNA, it was not possible to get a good fit for the repression of T7N by TetR. Therefore T7N was expressed as a function of arabinose.

network	changes compared to WT	engineered changes	expected changes from literature
I1 mutant1	$\beta_G = 1.0$	SP6 RNAP binding decreased	$\beta_G = 0.5$
mutant2	$\alpha_G = 0.95$	SP6 RNAP transcription initiation decreased	$\alpha_G = 1$
mutant3	$\alpha_l = 0.05$	concentration of active lacI strongly decreased	$\alpha_l = 0.04$
	$d = 0$ (fixed)		$d \approx 0$
I2 mutant1	$\alpha = 0.12$	weaker constitutive promoter	$\alpha = 0.41$
mutant2	$\beta = 0.41$	concentration of active TetR decreased	$\beta < 1$
mutant3	$\gamma = 6.5 \cdot 10^{-4}$	concentration of active lacI strongly decreased	$\gamma \approx 0$
I3 mutant1	$\beta_S = 2.04$	SP6 RNAP binding increased	$\beta_T = 2$
mutant2	$\beta_G = 0.26$	T7 RNAP binding decreased	$\alpha_G * \beta_G = 0.5$
mutant3	$\alpha_G = 0.63$	transcription initiation changed	
	$d = 0$ (fixed)	concentration of active lacI strongly decreased	$d \approx 0$
I4 mutant1	$\gamma = 0.41$	T7 RNAP binding decreased	$\gamma = 0.40$
mutant2	$\alpha_N = 0.008$	weaker constitutive promoter	$\alpha_N = 0.51$
mutant3	$\beta_N = 0.83$	concentration of active TetR strongly decreased	
	$T7N = a_N$ (fixed)	decreased	$T7N \approx a_N$
I0 mutant1	$\beta_T = 2.83$	concentration of active TetR increased	$\beta_T > 1$
mutant2	$d = 0$ (fixed)	concentration of active TetR strongly decreased	$d \approx 0$

Supplementary Table 7. Comparison of fitted changes to literature. Fitted changes are taken from Supplementary Tables 2-6. Also see Supplementary Fig. 7 for the engineered changes and Supplementary Table 9 for the literature values.

component	fit parameter	I0	I1	I2	I3	I4
T7p(-3G)	b (transcription)				4.43E+03	
	c (binding)				8.76E-02	
T7p(-14G)	b (transcription)				2.80E+03	6.25E+02*
	c (binding)				2.31E-02	3.33E-03*
SP6(WT)	b (transcription)		1.78E+03			
	c (binding)		1.00E+00			
SP6(-16G)	b (transcription)	1.65E+03	1.68E+03			
	c (binding)	2.26E-01	9.98E-01			
SP6(-6T)	bt (transcription)	1.65E+03			1.55E+03	
	ct (binding)	9.04E-02			3.57E-03	
SP6(-13T)	bt (transcription)				1.55E+03	
	ct (binding)				1.71E-03	
SP6(-11C)	bl (transcription)		4.85E+01#			
	cl (binding)		6.45E-02#			
SP6(-2G,-11C)	bl (transcription)		2.43E+00#			
	cl (binding)		6.45E-02#			

Supplementary Table 8. Comparison of fitted parameters across all networks. Parameters are taken from Supplementary Tables 2-6. They relate to the transcription and binding rates of the T7 and SP6 RNAP to their promoters (see Supplementary Table 1). Promoter mutations between nucleotides -17 to -5 (numbered relative to the transcription initiation site (+1)) affect mainly binding and mutations from nucleotides -4 to +6 affect mainly transcription initiation¹⁷. Parameters that are expected to be the same are underlayed with identical color and shade. Parameters that are affected by the promoter mutations are underlayed with the same color, but with a different shade: The darker the shading, the higher the expected value of the parameter. For the exact relation between the different promoters see Supplementary Table 9. Although each mechanism (I0-I4) has been fitted individually, all parameters involving T7 RNAP and SP6 RNAP are consistent throughout the networks. Slight deviations are in I4 where split T7 RNAP was used instead of T7 RNAP (marked with *) and in I1 where we observe a competition effect between the two SP6 promoters in the network (marked with #).

name	sequence	approximate relative activity
lacO	5' AATTGTTATCCGCTCACAATT	100% ^a
lacO(SymR+1)	5' AATTGTTATCCGGATAACAATT	40% ^a
lacO(SymL)	5' AATTGTGAGCGGCTCACAATT	4% ^a
TetO (O2)	5' TCCCTATCAGTGATAGAGA	100%
SP6p	5' ATTTAGGTGACACTATAG	100% ^b
SP6p(-16G)	5' AGTTAGGTGACACTATAG	45% ^b
SP6p(-6T)	5' ATTTAGGTGACTCTATAG	20% ^b
SP6p(-13T)	5' ATTTTGGTGACACTATAG	10% ^b
SP6p(-15G)	5' ATGTAGGTGACACTATAG	8% ^b
SP6p(-11C)	5' ATTTAGCTGACACTATAG	5% ^b
SP6p(-2G,-11C)	5' ATTTAGCTGACACTAGAG	<<5% ^b
T7p	5' TAATACGACTCACTATAG	100% ^c
T7p(-3G)	5' TAATACGACTCACTGTAG	21% ^c
T7p(-14G)	5' TAAGACGACTCACTATAG	10% ^c
T7p(-5T)	5' TAATACGACTCATTATAG	4% ^c
J23100	5' TTGACGGCTAGCTCAGTCCTAGGTACAGTGCTAGC	100% ^d
J23106	5' TTTACGGCTAGCTCAGTCCTAGGTATAGTGCTAGC	47% ^d
J23105	5' TTTACGGCTAGCTCAGTCCTAGGTACTATGCTAGC	24% ^d
J23114	5' TTTATGGCTAGCTCAGTCCTAGGTACAATGCTAGC	10% ^d
J23109	5' TTTACAGCTAGCTCAGTCCTAGGGACTGTGCTAGC	4% ^d

Supplementary Table 9. Sequences and relative activities of promoters and operators. Bold: transcription initiation site. a: taken from reference ⁶, b: taken from reference ⁷, c: taken from reference ¹⁷. Note that mutations between -17 to -5 affect mainly binding and mutations from -4 to +6 affect mainly transcription initiation¹⁷. d: taken from <http://partsregistry.org/Promoters/Catalog/Anderson>

AvrII_XhoI_f	5' CT CCTAGG ATGCAGTGAC CTCGAG ATGACGCTCTCCCTTATGCGAC
XhoI_AvrII_r	5' AT CTCGAG TCACTGCAT CCTAGG AGCAACCCAGTCAGCTCCTTCC
BglII_EcoRI_r	5' AT AGATCT TCACTGCAT GAATTC AGGGTATGGAGAAACAGTAGAGAGTTGC
AvrII_pBAD_f	5' GACTTAG CCTAGG GTCTGATTCGTTACCAATTATGACAAC
pBAD-BamHI T s	5' CATTTTT TATCCATAAGATTAGCGGT TCCTACCTGACGCTTTTT TATC
pBAD-BamHI T as	5' GATAAAA AGCGTCAGGTAGGA ACCGCTAATCTTATGGATAAAA ATG
lacI-f	5' GACTAGT CCATATG AAACCAGTAACGTTATACGATGTCG
lacI-r	5' CCTGCAGG GGATCCT TATTAAGGCCTTTATTAGGCGACCAGAGCATAGTTTTTCATCGT TAGCAGCAGGCCTCTGCCCGCTTTCCAGTC
TetR-f	5' GGCCG CGGTACCA AATAATTTTGTTTAACTTTAAGAAGGAGATATAC CATATG TCTA GATTAGATAAAAAGTAAAGTGATTAACAGC
TetR-r	5' CGCAGG GGATCCT TATTAAGGCCTTTATTAGGCGACCAGAGCATAGTTTTTCATCGTT AGCAGCAGGCCTGGACCCACTTTCACATTTAAGTTG
Split T7 N-f	5' GGTCACGTTTACAAA TAATAA GGATCCCCTGCAGGCCATGG
Split T7 N-r	5' CAGGGGATCCTTATT ATTTGTAAACGTGACCCACACG
Split T7 C-f	5' GGAGATATA CATATGAAAGCATTATGCAAGTGGTTGAAG
Split T7 C-r	5' TTGCATAAATGCTTT CATATGTATATCTCCTTCTTAAAGTTAAACAAAATTATTG

Supplementary Table 10. Sequences of primers used for cloning. Red: restriction sites, blue: complementary to target to be amplified.

for I1	
SP6p(-11C)_s	5' AATTC ATTTAGCTGACACTATA
SP6p(-11C)_as	5' CCCTTCTATAGTGTACAGCTAAAT G
SP6p(-2G,-11C)_s	5' AATTC ATTTAGCTGACACTAGA
SP6p(-2G,-11C)_as	5' CCCTTCTCTAGTGTACAGCTAAAT G
SP6p(WT)_s	5' AATTC ATTTAGGTGACACTATA
SP6p(WT)_as	5' CCCTTCTATAGTGTACCTAAAT G
SP6p(-16G)_s	5' AATTC CAGTTAGGTGACACTATA
SP6p(-16G)_as	5' CCCTTCTATAGTGTACCTAACT G
Spacer_B_s	5' GAAGGGGCCAAGCAGGGGGCCAAGCAGGGGGCCAAG GAGCT
Spacer_B_as	5' CCTTGG CCCCCTGCTTGGCCCCCTGCTTGGC
lacO(WT)_SP6p_s	5' GAAGGGAATTGTGAGCGGATAACAATTCC GAGCT
lacO(WT)_SP6p_as	5' CGGA AATTGTTATCCGCTCACAATT
for I2	
J23100_s	5' AATTC TTGACGGCTAGCTCAGTCCTAGGTACAGTGCTAGC
J23100_as	5' CCCTTCGCTAGCACTGTACCTAGGACTGAGCTAGCCGTCAAG G
J23114_s	5' AATTC TTTATGGCTAGCTCAGTCCTAGGTACAATGCTAGC
J23114_as	5' CCCTTCGCTAGCATTGTACCTAGGACTGAGCTAGCCATAAAG G
J23109_s	5' AATTC TTTACAGCTAGCTCAGTCCTAGGGACTGTGCTAGC
J23109_as	5' CCCTTCGCTAGCACAGTCCCTAGGACTGAGCTAGCTGTAAAG G
TetO_s	5' GAAGGGTCCCTATCAGTGATAGAGAG GAGCT
TetO_as	5' CTCT CTATCACTGATAGGGA
lacO(SymR+1)_SP6p_s	5' GAAGGGAATTGTTATCCGATAACAATTCC GAGCT
lacO(SymR+1)_SP6p_as	5' CGGA AATTGTTATCCGATAACAATT
for I3	
SP6p(-13T)_s	5' AATTC ATTTTGGTGACACTATA

SP6p(-13T)_as	5' CCCTTCTATAGTGTACCAAAAT G
SP6p(-6T)_s	5' AATTC ATTTAGGTGACTCTATA
SP6p(-6T)_as	5' CCCTTCTATAGAGTCACCTAAAT G
T7p(-3G)_s	5' AATTC TAATACGACTCACTGT
T7p(-3G)_I3_as	5' TCCCCTACAGTGAGTCGTATTAG G
T7p(-14G)_s	5' AATTC TAAGACGACTCACTAT
T7p(-14G)_I3_as	5' TCCCCTATAGTGAGTCGTCTTAG G
Spacer_B_s	5' GAAGGGGCCAAGCAGGGGGCCAAGCAGGGGGCCAAG GAGCT
Spacer_B_as	5' CCTTGG CCCCCTGCTTGGCCCCCTGCTTGGC
lacO(SymR+1)_T7p_s	5' AGGGGAATTGTTATCCGGATAACAATTCC GAGCT
lacO(SymR+1)_T7p_as	5' CGGA ATTGTTATCCGGATAACAAT
for I4	
J23106_s	5' AATTC TTTACGGCTAGCTCAGTCCTAGGTATAGTGCTAGC
J23106_as	5' CCCTTCGCTAGCACTATACCTAGGACTGAGCTAGCCGTAAAG G
J23105_s	5' AATTC TTTACGGCTAGCTCAGTCCTAGGTACTATGCTAGC
J23105_as	5' CCCTTCGCTAGCATAGTACCTAGGACTGAGCTAGCCGTAAAG G
TetO_s	5' GAAGGGTCCCTATCAGTGATAGAGAG GAGCT
TetO_as	5' CTCT CTATCACTGATAGGGA
T7p(-14G)_s	5' AATTC TAAGACGACTCACTAT
T7p(-14G)_as	5' CCCTTCTATAGTGAGTCGTCTTAG G
T7p(-5T)_s	5' AATTC TAATACGACTCATTAT
T7p(-5T)_as	5' CTCCCTATAATGAGTCGTATTAG G
Spacer_A_s	5' AGGGAGGCTGCTGCTGCTGCTGCTGCTGCTGCTGCT GAGCT
Spacer_A_as	5' CAGC AGCAGCAGCAGCAGCAGCAGCAGCAGCAGC
for I0	
SP6p(-6T)_s	5' AATTC ATTTAGGTGACTCTATA

SP6p(-6T)_as	5' CCCTTCTATAGAGTCACCTAAAT G
SP6p(-16G)_s	5' AATTC AGTTAGGTGACACTATA
SP6p(-16G)_as	5' CCCTTCTATAGTGTCACCTAACT G
TetO_s	5' GAAGGGTCCCTATCAGTGATAGAGAG GAGCT
TetO_as	5' CTCTCT ATCACTGATAGGGA
for I2+	
SP6p(-15G)_s	5' AATTC ATGTAGGTGACACTATA
SP6p(-15G)_as	5' CCCTTCTATAGTGTCACCTACAT G
J23100_s	5' AATTC TTGACGGCTAGCTCAGTCCTAGGTACAGTGCTAGC
J23100_as	5' CCCTTCGCTAGCACTGTACCTAGGACTGAGCTAGCCGTCA AG
TetO_s	5' GAAGGGTCCCTATCAGTGATAGAGAG GAGCT
TetO_as	5' CTCTCT ATCACTGATAGGGA
lacO(SymL)_SP6p_s	5' GAAGGGAATTGTGAGCGGCTCACAATTCC GAGCT
lacO(SymL)_SP6p_as	5' CGGA ATTGTGAGCCGCTCACAATT

Supplementary Table 11. Sequences of oligonucleotides for promoters and operators. Red: overhang complementary to restriction site.

Seq_0_f	5' GAGTTGTAAAACGACGGCCAG
Seq_1_f	5' GTTGAGTTACCTGCAGCGATTG
Seq_1_r	5' CAATCGCTGCAGGTA ACTCAAC
Seq_2_f	5' CAATCGCTTGGACCAGCTTTC
Seq_2_r	5' GAAAGCTGGTCCAAGCGATTG
Seq_3_f	5' CTCATTCGCTAATCGCCAC
Seq_3_r	5' GTGGCGATTAGCGAATGAG
Seq_4_r	5' GCTAGTTATTGCTCAGCGGTG
pET_Seq	5' CTCATGAGCGGATACATATTTGAATG
pCDF_Seq	5' CACCTGAAGTCAGCCCCATAC
pCOLA_Seq	5' GCCGTCACTGCGTCTTTTAC
pUC_f	5' GCATCAGAGCAGATTG TACTGAG
pUC_r	5' CGTATGTTGTGTGGAATTGTGAG

Supplementary Table 12. Sequences of primers used for sequencing.

qPCR_sfGFP_f	5' TGAAATTCGAAGGCGATACC
qPCR_sfGFP_r	5' TGTTTATCCGCGGTGATGTA
qPCR_T7RNAP_f	5'GATGTTTCAGCCGTGTGTTG
qPCR_T7RNAP_r	5' CATCTTCATAGCGCATCAGC
qPCR_SP6RNAP_f	5' TCGTGGATGAAGCAGCTATG
qPCR_SP6RNAP_r	5' ATCACTGCAATGCTCGTCAC
qPCR_hsvTK(spike)_f	5' TCCCATGCACGTCTTTATCC
qPCR_hsvTK(spike)_r	5' ACCATCCCGGAGGTAAGTTG
qPCR_lacI_f	5' TGGTGGTGTTCGATGGTAGAA
qPCR_lacI_r	5' CTGGTCATCCAGCGGATAGT
qPCR_TetR_f	5' AAAATAAGCGGGCTTTGCTC
qPCR_TetR_r	5' GCCAGCTTTCCCCTTCTAAA
qPCR_pCOLA_lacI_s	5' CGAATTCATTTACCCAAGG
qPCR_pCOLA_lacI_as	5' GGCATACTCTGCGACATCGT
qPCR_pCDF_lacI_s	5' CACCACCTGCAGGACCTC
qPCR_pCDF_lacI_as	5' GGCATACTCTGCGACATCGT
qPCR_T7RNAP N split_f	5' CGGAAGCTGTGGCGTATATT
qPCR_T7RNAP N split_r	5' TTCATCTTCGATTGCACGAC

Supplementary Table 13. Sequences of qPCR primers.

Supplementary Methods

A) Computational Methods

Complexity atlas

We have performed a computational exploration of all 3-gene networks that are capable of transforming an input gradient into a stripe of gene expression. For this purpose we employed a simulation code build in-house⁸. Resuming the assumptions and approximations of Cotterell and Sharpe⁸, we consider that one of the three genes receives the input, and that a set of random parameters is functional if at least one of the genes produces a single-stripe expression. For the current study, a few modifications have been considered with respect to the previous study⁸. These modifications are as follows:

- Self-inhibitions are not considered, because they do not introduce a qualitative change in the stripe-formation process⁹.
- There is no diffusion of the gene's products outside the cell, because our synthetic networks are composed of cell-autonomous factors.
- To limit the number of parameters in this extensive exploration, the production rate from any gene g is defined as follows:

$$\begin{aligned}\frac{dg}{dt} &= \frac{1}{[1 + (cX)^n][1 + (dY)^n][1 + (kZ)^n]} \text{ if } X, Y, Z \text{ are inhibitors} \\ &= \frac{0.01 + (cX)^n}{[1 + (cX)^n][1 + (dY)^n][1 + (kZ)^n]} \text{ if only } X \text{ is activating} \\ &= \frac{0.01 + (cX)^n(dY)^n}{[1 + (cX)^n][1 + (dY)^n][1 + (kZ)^n]} \text{ if } X \text{ and } Y \text{ are activating}\end{aligned}$$

(1)

where the binding constants c , d and k take random and uniform values $\in [0, 1 = \text{MaxConcentration}]$ with $\text{MaxConcentration} = 1/\delta$, and $\delta = 0.05$ fixed value for the degradation rate. Notice that we consider the same exponent for all genes, and more precisely its value is $n = 2$. The value 0.01 in the nominators constitutes a low basal level. In the case a gene receives no activating input, this low basal acquires a high value, that is 1, and the promoter is thus considered constitutive.

- The input (morphogen) has a distribution given by $M = Id^C$, with $I = 10$, $d = 0.93$, and C the cell number $\in [1, 52]$. The binding constant for the morphogen to the genes is constant for all genes and equal to 3.
- Here, we define a stripe as a region of at most 36 cells of high expression, preceded and followed by a region of low expression, where “low” refers to values lower than 30% of MaxConcentration , and “high” refers to values higher than 30% of MaxConcentration .

- The number of solutions that each topology has is a measure of its mutational robustness (Supplementary Fig. 2). A network must have at least one solution to be considered functional.

The assumptions of the current model, the introduction of constitutive promoters and AND-type signal integration produce inherent differences in the resultant complexity atlas when compared to the one from our previous work⁸.

The fitting software

ROOT¹⁰ (root.cern.ch) is an object-oriented framework that has a C/C++ interpreter (CINT) and C/C++ compiler (ACLIC). Developed at CERN, ROOT is used extensively in High Energy Physics for “data analysis”, reading and writing data files, and calculating a wide range of embedded statistical procedures. As a free and C++-based analysis software, it allows the user to put together and combine the fitting functions and methods provided by ROOT into an analysis code specifically adapted to the particularities of the problem studied. Among the myriad of functionalities of ROOT, we have employed mainly the fitting histograms and data points, together with the associated 2D visualization tools. Fitting in ROOT is based on the Minuit package that provides Maximum Likelihood Estimates through Local Optimization (root.cern.ch/root/html/TMinuit.html). It includes fitting nonlinear functions with limits on variable parameters and reliability measures on error estimates.

We have chosen to employ the ROOT platform for the fitting procedure and develop a battery of methods adapted to the experimental procedures and the resultant data features. We have synthetically built and subsequently modeled 5 topologies of genetic circuits (Fig. 4-6 and Supplementary Fig. 7). For each topology, we have built several constructs distinguishable by certain controlled mutations (Fig. 5-6 and Supplementary Fig. 7). Within the mathematical model associated to the genetic circuit, and thus within the fitting procedure, the distinct constructs associated to the same topology share certain parameters, while varying others. Due to this particularity, we have developed an analysis procedure that collectively fits the data associated to a given topology by defining a combined likelihood function. In the following, we describe the mathematical model and the collective likelihood function employed.

The model

For the fitting of the experimental data, we have employed a Hill-like function kinetic model¹¹ for characterizing the gene-regulation function. While more general gene-regulation frameworks exist¹², we have chosen to employ the current kinetic model for being widely and successfully used in the description of prokaryotic¹³ and even mammalian regulation¹⁴, and for being subject to the analytical and simulation tools of nonlinear ODEs. We describe the model in Supplementary Fig. 1. Within the generality of the model, we have specifically defined the parameters of the models in terms of phenomenological rate constants and other physical parameters (Supplementary Table 1) in order to allow for a direct comparison of the inferred rate constants across the constructed networks, and eventually with known values from the literature.

Let us consider as an example an activator X and an inhibitor Y regulating the expression of gene Z (Supplementary Fig. 1). If the level of mRNA can be measured for X , Y and Z , then we expect the mRNA level of Z to be given by Eq. (2) (Supplementary Fig. 1) where X , Y and Z are the number of mRNA

molecules per cell, and the constants are defined as follows: a – the basal transcription rate; b – transcription rate for the active form; e – transcription rate when both the activator and the inhibitors are bound; c – the binding constant for the activator X ; d – the binding constant for the inhibitor Y ; f – cooperativity factor indicating whether X and Y have a positive cooperativity ($f > 1$) or a negative cooperativity ($f < 1$). The exponents n and m generally referred to as Hill coefficients reflect the multimerization of X and Y , respectively, multiple binding sites or titration/sequestration effects¹⁵. In the experimental framework employed in this study, the exponents are generally $n = 1$ for the activators (SP6 RNAP, T7 RNAP) and $m \in [1, 4]$ for the repressors (lacI, TetR). When titration effects are expected, such coefficients can take higher values¹⁵. The detailed definitions of the parameters are in Supplementary Table 1.

$$Z(X, Y) = \frac{a + b(cX)^n + e(cX)^n(dY)^m}{1 + (cX)^n + (dY)^m + (cX)^n(dY)^m} \quad (2)$$

We wish to point out that the Hill-like function (Eq. 2) (Supplementary Fig. 1) naturally allows for constitutive promoters (high value of parameter a) and for a fine tuning of the degree between OR- and AND-gates (the parameters e and f). In order to provide the direct relation to biological meaning that we aimed at, the function has many biologically-relevant free parameters (i.e. 3 parameters per link, compared to 1 parameter per link as in the connectionist case of the previous work⁸). The experimental constructs involved 3-link 3-gene incoherent feed-forward motifs, where thus a gene could have at most two inputs. However, the large scale exploration of the complexity atlas included more complex networks, and thus more parameters. For this reason, we fixed the values of some of these parameters for the numerical simulations of the complexity atlas. For example, the above two-input function in Eq. (2) would appear in the simulated atlas as:

$$Z(X, Y) = \frac{a + b(cX)^n + e(cX)^n(dY)^m}{[1 + (cX)^n][1 + (dY)^m]} = \frac{a + b(cX)^n + e(cX)^n(dY)^m}{1 + (cX)^n + (dY)^m + (cX)^n(dY)^m} \quad (3)$$

where $f=1$ and a, b, e have fixed values depending on the nature of X and Y (both activators, both inhibitors, or distinct). In other words, while the complexity-atlas model and the synthetic-constructs model share similar mathematical expressions, the latter has more degrees of freedom than the former. We expect that a complexity atlas of more free parameters would show a higher degree of connectedness, but would require substantially longer simulation time.

The fitting procedure

The experimental protocols and the mutant constructs associated to each of the 5 genetic circuits allow us to determine the parameters of the regulation function for the individual interactions. This is to say, the collected data allow each interaction of the type $A \rightarrow B$, where \rightarrow implies either activation or inhibition, to be fitted to a Hill function and the associated parameters obtained. The feedforward nature of the genetic circuits built, allows us to fit the data at steady state (Eq. 7-9), instead of requiring the modeling and associated fitting of the full ordinary differential equations (Eq. 4-6). Let us consider the steady-state

approximation in detail for the case of the archetype network IO as the simplest network of our study. In this case, the full systems describing the temporal evolution of the concentrations of TetR, SP6 RNAP and GFP is:

$$\frac{dTetR}{dt} = \frac{\tilde{a}_T + \tilde{b}_T (c_T ara)^{n_T}}{1 + (c_T ara)^{n_T}} - \delta_T TetR \quad (4)$$

$$\frac{dSP6}{dt} = \frac{\tilde{a}_S + \tilde{b}_S (c_S ara)^{n_S}}{1 + (c_S ara)^{n_S}} - \delta_S SP6 \quad (5)$$

$$\frac{dGFP}{dt} = \frac{\tilde{a} + \tilde{b}(c SP6)^n + \tilde{e}f(c SP6)^n(d TetR)^m}{1 + (c SP6)^n + (d TetR)^m + f(c SP6)^n(d TetR)^m} - \delta_G GFP \quad (6)$$

At steady state, the values of the concentrations are given by:

$$TetR = \frac{\frac{\tilde{a}_T}{\delta_T} + \frac{\tilde{b}_T}{\delta_T} (c_T ara)^{n_T}}{1 + (c_T ara)^{n_T}} = \frac{a_T + b_T (c_T ara)^{n_T}}{1 + (c_T ara)^{n_T}} \quad (7)$$

$$SP6 = \frac{\frac{\tilde{a}_S}{\delta_S} + \frac{\tilde{b}_S}{\delta_S} (c_S ara)^{n_S}}{1 + (c_S ara)^{n_S}} = \frac{a_S + b_S (c_S ara)^{n_S}}{1 + (c_S ara)^{n_S}} \quad (8)$$

$$GFP = \frac{a + b(c SP6)^n + ef(c SP6)^n(d TetR)^m}{1 + (c SP6)^n + (d TetR)^m + f(c SP6)^n(d TetR)^m} \quad (9)$$

Several constructs have been built for the archetype 2-node topology distinguishable by mutations at specific interactions. These are enumerated in Supplementary Table 2, illustrating that several parameters are shared among constructs. Due to this feature, we consider it appropriate to define a combined likelihood function that collectively produces a fit for all constructs. This likelihood function \mathcal{L} is defined through the parameters from Supplementary Table 2 as follows:

$$\begin{aligned} \mathcal{L}(a_S, b_S, c_S, n_S, a_T, b_T, c_T, n_T, a, b, c, d, e, f, n, m, \beta_T) = \\ \mathcal{L}_S(a_S, b_S, c_S, n_S) + \mathcal{L}_T(a_T, b_T, c_T, n_T) + \mathcal{L}_{GFPWT}(a, b, c, d, e, f, n, m) + \\ \mathcal{L}_{GFPmut1}(a, b, c, n) + \mathcal{L}_{GFPmut2}(a, b, c, d, e, f, n, m, \beta_T) \end{aligned} \quad (10)$$

Where

$$\mathcal{L}_S(a_S, b_S, c_S, n_S) \equiv \sum_{i=0}^N \left[\frac{SP6_{observed} - SP6_{theoretical}}{\sigma_i} \right]^2 \quad (11)$$

with N , the total number of experimental points, and σ_i , the standard deviation of the measurement i in the concentration of SP6 RNAP. Similar definitions are \mathcal{L}_T for the TetR data, $\mathcal{L}_{GFPmut1}$ for the GFP data of mutant 1, and so forth. The algorithm MIGRAD from the Minuit package of the ROOT software searches for the values of the parameters that minimize the total \mathcal{L} defined in Eq. (10). In addition to the definition of the parameters in Supplementary Fig. 1, the greek letters α , β , γ are used for the mutant networks. They are non-dimensional factors that multiply parameters of the WT circuit. As an example, the factor β_T for the archetype in Eq. (10) multiplies the binding parameter d of the TetR for mutant 1. In this case, it is expected from the literature that $\beta_T > 1$ (Supplementary Table 7).

For all 5 genetic circuits, we have one construct for which we measure the mRNA/cell for all nodes, in addition to the fluorescence levels of the GFP node. From these data, we can establish an equivalence relation between mRNA/cell and the fluorescence levels of the GFP. While for the rest of the constructs associated to the same topology we have measured only fluorescence levels, we employ this equivalence relation to transform all fluorescence data into mRNA/cell. In so doing, the parameters defined in Supplementary Table 2 of the archetype example have the biological meaning defined in Supplementary Table 1.

Finally, within the fitting protocol, we have applied the following 3-step procedure:

1. Within each topology, we fit a linear equivalence relation between both RNA/cell and fluorescence levels for those constructs for which we have measured both RNA/cell and fluorescence levels. We employ this relation to transform the fluorescence data into RNA/cell data for the rest of the constructs. In the subsequent fitting procedures, all data consist in RNA/cell for all genes.
2. We individually fit each interaction to determine the parameters of the Hill-function (one-input interactions) and Hill-like function equation (2) (two-input interactions).
3. After establishing the interval for the parameters' values from these individual fittings, we perform a collective fit of all constructs within one topology using a combined likelihood function equivalent to Eq. (10). The collective fit imposes the parameters to be common among the constructs. The input into the collective fit is the concentration of arabinose, and the output consists in the expected behavior of all "nodes" of the network, and the associated parameters of the regulation function.

Comparison of feed-forward loops from the complexity atlas and the experiments

Figure 1 in the main text includes the phase portraits of the 4 incoherent feed-forward networks, illustrating the dynamical process of stripe formation through the movement of nullclines and thus steady states. While schematic, the 4 cases correspond to 4 specific networks with particular parameter values as they resulted from the complexity atlas simulations. In order to establish a mechanistic process of stripe formation and a direct relation between the regulation function used in atlas simulations and the one used for data fitting, we analytically establish the movement of the green nullcline as the morphogen changes. In other words, we show that the same mechanism of stripe formation (i.e. movement of nullclines under the morphogen gradient) occurs in both models using I1 and I3 as example. Supplementary Fig. 8 shows the calculated nullclines for I1 and I3 using the fitted parameters (Supplementary Table 3 and Supplementary Table 5; respectively) of the synthetic circuits. They are qualitative the same as the nullclines calculated from the complexity atlas (Fig. 1).

For the I1 network (Supplementary Fig. 8a), we draw a phase portrait that shows GFP (or gene B) versus the repressor (lacI, gene C). In order to understand how the GFP nullcline moves under the change in morphogen, we re-write the formula of Eq (2) considering the protein A (SP6 RNAP) as a constant:

$$GFP(C)_A = \frac{[a + b(cA)^n] + [ef(cA)^n](dC)^m}{[1 + (cA)^n] + [1 + f(cA)^n](dC)^m} = \frac{\alpha(A) + \beta(A)(dC)^m}{\gamma(A) + \delta(A)(dC)^m} \quad (12)$$

This tells us that the green curve $GFP(C)$ has the shape of a Hill function whose constants (height and threshold point) depend on A . The height of the green nullcline when the repressor is zero ($C=0$) is given by

$$GFP(C = 0)_A = \frac{\alpha(A)}{\gamma(A)} = \frac{a + b(cA)^n}{1 + (cA)^n} \quad (13)$$

Therefore, the green nullcline at $C=0$ has a height approximated by the value of the parameter a when A is small, and by the value of the parameter b when A is large. Consequently, from the values of the parameters (Supplementary Table 3), the height of the green nullcline increases as the morphogen and thus A increase, i.e. measured at $C=0$, the green nullcline extends upwards as arabinose the increases.

For the I3 network (Supplementary Fig. 8a) we calculate a phase portrait that shows GFP (or gene B) versus the activator (T7 RNAP, gene C). In order to understand how the GFP nullcline moves when the morphogen changes, we re-write the formula from Eq. 2 considering the protein A (lacI) as a constant:

$$GFP(C)_A = \frac{a + [b + ef(dA)^m](cC)^n}{[1 + (dA)^m] + [1 + f(dA)^m](cC)^n} = \frac{\bar{\alpha}(A) + \bar{\beta}(A)(cC)^n}{\bar{\gamma}(A) + \bar{\delta}(A)(cC)^n} \quad (14)$$

which tells us that the green curve $GFP(C)$ has the shape of a Hill function whose constants (height and threshold point) depend on A . The basal of this sigmoidal is:

$$GFP(C = 0)_A = \frac{a}{1 + (dA)^m} \quad (15)$$

The height or maximum value of the green nullcline when the activator C is large is given by

$$GFP(C: large)_A = \frac{\bar{\beta}(A)}{\bar{\delta}(A)} = \frac{b + ef(dA)^m}{1 + f(dA)^m} \quad (16)$$

telling us that for low inhibitor A (low arabinose), the height is equal to the parameter b , while for high A (high arabinose), it decrease towards the value of parameter $e < b$.

B) Experimental Methods

Materials

Restriction enzymes and T4 DNA ligase were purchased from New England BioLabs (NEB). Oligonucleotides and chemicals (unless otherwise stated) were ordered from Sigma-Aldrich.

Media

Cloning steps used 1 × Luria-Bertani medium (LB: 10 g Bacto-tryptone, 5 g yeast extract, 10 g NaCl per 1 l), with appropriate antibiotic. Stripe experiments used 'Stripe Medium' (SM: 1 × LB plus 0.4% (w/v) glucose, 50 µg/ml ampicillin, 15 µg/ml kanamycin and 25 µg/ml spectinomycin). Spectinomycin was omitted for the I0 network, and 0.75 × LB was used for the I1 network.

Cloning

Restriction digests and ligations were performed with standard protocols¹⁸. Chemically competent TOP10 cells (Invitrogen) were used for subcloning. Plasmids were purified using QIAprep Spin Miniprep Kit (QIAGEN).

Network scaffold

Overview

The three nodes of the network are contained in three compatible plasmids (pCOLA, pCDF, pET) each containing a multiple cloning site (MCS) for subcloning of the individual components and a set of transcriptional terminators (Fig. 2). The plasmids contain different origins of replication (ori: ColA, CDF and pRB322) each with 20-40 copies per cell (Novagen user protocol TB055 Rev. C 0611JN) and antibiotic resistances (kanamycin, spectinomycin and ampicillin). The pCOLA plasmid constitutively expresses AraC and contains the P_{BAD} promoter¹⁹. Therefore, the expression of genes cloned into this plasmid is induced by arabinose. The pET plasmid contains GFP (with a LVA degradation tag³) for the fluorescent readout.

Plasmids

Plasmids pET-17b, pCDF-1b, pCOLA-Duet-1 were purchased from Novagen. lacI was removed from pCDF-1b and pCOLA-Duet-1 by PCR²⁰ using the primers AvrII_XhoI_f and Xho_AvrII_r. These primers also introduced the restriction sites AvrII and XhoI. A multiple cloning site (MCS) was designed (Supplementary Fig. 8) and chemically synthesised (GenScript). The MCS was ligated into pET-17b (via BglII, AatII), pCDF-1b and pCOLA-Duet-1 (via XhoI, AgeI). AraC and the P_{BAD} promoter were amplified from pBAD202 (Invitrogen) with the primers BglII_EcoRI_r and AvrII_pBAD_f and cloned into pCOLA-MCS (via AvrII, EcoRI). A BamHI restriction site in front of the P_{BAD} promoter was removed by mutating one base pair (A→T) with the primers pBAD-BamHI T s and pBAD-BamHI T as.

Genes

All genes are “stored” in pUC57 plasmids, ready to be subcloned into the plasmid scaffolds by cutting with the respective restriction enzymes, followed by ligation. The genes are preceded by a ribosome binding site

(RBS), an enhancer (epsilon sequence) and have an NdeI site at their start codon. Genes are flanked 5' by the restriction sites SalI, NotI and KpnI, and 3' by the restriction sites BamHI, SbfI and NcoI. An example (GFP-LVA) is shown in Supplementary Fig. 12.

All genes contain a degradation tag. The T7 RNA polymerase (RNAP) and SP6 RNAP contain an N-terminal “UmuD” tag. It is composed of the first 29 amino acids of the SOS mutagenesis protein UmuD, with a linker (2×GGGS), and targets associated proteins for Lon-mediated proteolysis^{4,21}. The remaining genes contain a C-terminal “LVA” *ssrA* tag³. The UmuD tags are flanked by two NdeI sites and the LVA tags by two StuI sites, allowing easy removal of the tags if required.

UmuD-T7 RNAP, UmuD-SP6 RNAP and superfolder GFP-LVA², were codon-optimized and synthesized by GenScript. Duplicate cloning restrictions sites were excluded. LacI was PCR-amplified from pCDF-1b with the primers lacI-f and lac-r. The primers introduced a 5' NdeI site, a C-terminal LVA-tag and a 3' BamHI site. TetR was PCR-amplified from pcDNA6/TR (Invitrogen) with the primers TetR-f and TetR-r. The primers also introduced 5' KpnI and NdeI sites, a C-terminal LVA-tag and a 3' BamHI site. All genes were cloned into pUC57 containing the generic flanking sequences (Supplementary Fig. 11). Split T7 RNAP⁵ was cloned²⁰ from the codon-optimized UmuD-T7 RNAP in pUC57: The N-terminal fragment (UmuD-T7 RNAP N) was PCR-amplified with the primers Split T7 N-f and Split T7 N-r. The primers also introduced two stop codons. The C-terminal fragment (T7 RNAP C) was PCR-amplified with the primers Split T7 C-f and Split T7 N-r. The primers also introduced an ATG start codon.

Promoters and repressor binding sites

Promoters and repressor binding sites were ordered as oligonucleotides. The promoter oligonucleotides contain a EcoRI site overhang at the 5' end and a 6 nt long overhang at the 3' end. The repressor binding site oligonucleotides contain an overhang matching the promoter at the 5' end and a SacI site overhang at the 3' end. If no functional repressor binding site was required, the oligonucleotides termed Spacer_A were ligated to the T7 promoters and the oligonucleotides termed Spacer_B were ligated to the SP6 and constant promoters.

The oligonucleotides were phosphorylated with T4 polynucleotide kinase (NEB). The sense and antisense oligonucleotides were annealed by heating to 95 °C and cooling slowly to room temperature. The annealed oligonucleotides were ligated into the plasmid scaffold, in between EcoRI and SacI.

The sequences and relative activities of the SP6 promoter⁷, T7 promoter¹⁷ and constitutive promoter variants (<http://partsregistry.org/Promoters/Catalog/Anderson>), as well as of lacI operator site variants⁶, were taken from the literature (Supplementary Table 9).

E. coli strain

A descendant of strain BW27783²² was used. In BW27783²² the native *araE* promoter is replaced by a constitutive promoter. This results in a homogeneous cell population expressing genes under the control of the P_{BAD} promoter, with a graded response to arabinose. In addition, in the strain used, lacI (ECK0342) was replaced by a chloramphenicol resistance gene (strain MK01²³) and *tdk* (ECK1233) was removed as previously described²⁴.

The cells were made electrocompetent and aliquots were stored at -80 °C. The three plasmids (pCOLA, pCDF and pET) were transformed simultaneously using a Bio-Rad gene pulser Xcell electroporator. Transformed bacteria were plated out on stripe medium-agar plates. Glycerol stocks were prepared for long-term storage of transformed cells.

Fluorescence measurements on agar plate

For the detection of fluorescence from cells grown on an agar plate, we adapted previously-described protocols^{25,26}. Briefly, a single colony was picked and grown overnight in 5 ml SM ("Stripe Medium"). The optical density (OD) at 600 nm was measured and the culture was diluted to OD 0.15 in SM. 400 µl of the diluted culture were spread evenly over an SM-agar (1.5%, 20ml) Petri dish (90 mm diameter). The SM-agar contained 15 µM IPTG for I2 and 0.2 µM aTc for I0 (stripe). The plates were incubated at 37 °C for 1 h. Subsequently, a dry 1 cm diameter autoclaved paper disc was placed at the centre of the plate and 15 µl of 5% (w/v) arabinose were injected onto the disc. The plates were incubated at 37 °C for another 6 h (5 h for the I0 antistripe network). Fluorescence images were acquired with a Typhoon Trio imager (GE Lifescience) using 488 nm laser excitation and 526 nm short pass filter detection; 200 µm resolution and agar top focusing (+3 mm). Grayscale images were converted to green using Image Quant TL software (GE Lifescience). The contrast was enhanced by using the curves function of Photoshop.

Absorbance and fluorescence measurements

A single colony was picked for each biological replicate and grown overnight in 5 ml "Stripe Medium" (SM). The optical densities (OD) at 600 nm were measured and the cultures were diluted to OD 0.0015 in SM (containing IPTG or aTc when indicated). 120 µl of the diluted culture and 2.4 µl of arabinose at 16 different concentrations (two-fold serial dilution) were added to the wells of a 96-well plate (BD 351172). Arabinose concentration ranges: 0-0.1% (w/v) for I1, I3, I0; 0-0.2% for I2; 0-0.4% (w/v) for I4. The absorbance at 600 nm and green fluorescence (excitation: 485 nm, emission: 520 nm) were measured every 6 min in a Tecan Infinite M200 plate reader (Infinite M200 Pro for I3) until the *E. coli* cells reached stationary phase (6 h for I1-I4, 5 h for I0). The temperature was 37 °C and, between readings, the plate was shaken for 220 s (orbital, 2 mm). A different gain of the fluorescence measurement was chosen for each stripe-mechanism (I1, I2, I3, I4, I0), but the same gain was then used for all mutants of one mechanism. The plates were incubated and read with their lids on to reduce evaporation. To avoid edge-effects only the central 60 wells of each plate were used (the remaining wells were filled with sterile SM). All measurements were obtained from three independent biological replicates, maintained simultaneously under identical conditions. For each experiment, control cells transformed with the empty plasmids (pCOLA-MCS, pCDF-MCS and pET-MCS for I1-I4, pCOLA-MCS and pET-MCS for I0) and were grown on the same plate. 6 control wells, containing only SM, were also measured at each time point and were used for background subtraction.

The background fluorescence of the stripe medium was subtracted from the sample fluorescence. Identically, the background absorbance was subtracted from the sample absorbance. The background-corrected fluorescence was then normalized for the number of cells by dividing by the background-corrected absorbance. The background corrected normalized fluorescence at 6 h of growth (5 h for I0) are shown. In

Fig. 4 the dynamics of the fluorescence over the last 1 h (2 h for I1) of growth are shown. The average of 3 biological replicates and standard deviations were plotted.

Re-growth for the exclusion of inactivating mutations

Cells were grown in the Tecan plate reader as described in the section “Absorbance and fluorescence measurements”. For each replicate, 1 µl of the cultures grown either at 0% arabinose or at the highest arabinose concentration were diluted into 5 ml SM and grown overnight. Additional three colonies were picked from the agar plate and also grown overnight in 5 ml SM. The second round of absorbance and fluorescence measurements was performed as described above, with the change that the cells were assayed at 6 representative arabinose concentrations instead of 16.

RNA extraction

Cells were grown in the Tecan plate reader as described in the section “Absorbance and fluorescence measurements”. 100 µl RNaProtect Bacteria Reagent (QIAGEN) were added to 50 µl cells. The samples were mixed, incubated and centrifuged according to the manufacturer's instructions. The cell pellets were stored at -80 °C until further processing. RNA was extracted using the Maxwell 16 LEV simplyRNA tissue kit (Promega). Briefly, the pellets were resuspended in 100 µl lysozyme (1 mg/ml in TE buffer, pH 8.0) and shaken for 5 min at RT. 100 µl of homogenisation solution (including 1-thioglycerol) were added, followed by 200 µl of lysis buffer. 2 ng of spike RNA and the cell lysates were transferred to the Maxwell cartridge and the remaining steps were performed by the Maxwell 16 instrument using the program “simply RNA”. The RNA was eluted in 30 µl of water. The concentrations were determined by Nanodrop (ThermoScientific). The RNA was stored at -80 °C.

Reverse transcription (RT)

700 ng of RNA was treated with Deoxyribonuclease I, Amplification Grade (Invitrogen) according to the manufacturer's instructions. 8 µl of this reaction was directly used for reverse transcription using SuperScript III First-Strand Synthesis SuperMix for qRT-PCR (Invitrogen). The reaction was performed according to the manufacturer's instructions, except omitting digestion of the RNA with RNase H.

Quantitative PCR (qPCR)

RNA transcripts were quantified in a 10 µl RT-qPCR reaction, containing 2 µl of 10- to 200-fold diluted cDNA sample, 0.25 µM final concentration of forward and reverse primers and 5 µl of LightCycler 480 SYBR Green I Master (Roche). RT-qPCR reactions were run on a LightCycler 480 System (Roche) in 384 well plates: denaturation (95 °C, 8 min, 4.8 °C/s); 45 cycles of amplification (95 °C, 10 s, 4.8 °C/s; 59 °C, 30 s, 2.5 °C/s; 72 °C, 10 s, 4.8 °C/s); melting (95 °C, 30 s, 4.8 °C/s; 65 °C, 1 min, 2.5 °C/s; 98 °C, 0.11 °C/s); annealing and cooling (59 °C, 10 s, 2.5 °C/s; 72 °C, 2 min, 4.8 °C/s, 40 °C, 30 s, 2 °C/s). All Primer sets were tested for specificity by melting curve and gel analysis. Each run also included positive controls with a known amount of the linearized plasmid and two negative controls (with no template and without reverse transcription). Primers were designed using Primer3Plus software²⁷ and sequences are given in Supplementary Table 13. Three biological replicates were measured for each condition. Each qPCR was

carried out at least in technical duplicate. DNA amounts were determined with the help of a standard ladder of known quantities of the corresponding BglII-linearized plasmid. Data were analyzed with LightCycler 480 software 1.5.0 with the “Abs Quant/2nd Derivative Max” analysis function.

Normalization per cell

To obtain an estimate of mRNA copy numbers per cell²⁸ the cell lysates were spiked with a known amount (2 ng) of external RNA. The spike RNA (2630 nt) was produced using the MEGAscript T7 kit (Ambion Inc.). The template for transcription was a linearized pET-MCS plasmid containing the WT T7 promoter and 2 genes (hsvTK and a synthetic zinc finger). The mRNA was purified according to the RNeasy MinElute protocol (QIAGEN). Quality was monitored with a 2100 bioanalyzer (Agilent). Initially, the dose-response linearity was verified to ensure that the recovery of the spike RNA is linear in the range of concentrations of our samples (Supplementary Fig. 14).

The number of spike molecules was measured by qPCR as described above. A recovery rate of the spike through the process of RNA extraction, reverse transcription and qPCR was calculated by dividing the measured output amount by the input amount. The measured amounts of mRNA of the other genes were divided by the recovery rate to obtain the initial amounts of mRNA copies per sample. To calculate the number of mRNA copies per cell, this number was divided by the number of cells present in a particular sample. The number of cells per sample was calculated from the measured absorbance. In order to be able to correlate the absorbance measured by the Tecan plate reader to the number of bacteria in a sample, initially a standard curve of serial dilutions was generated and plated for viable counts. The measured absorbance was plotted versus the colony forming units (CFU). Linear regression yielded the following relation: $\text{CFU/ml} = 1.872 \cdot 10^9 \cdot \text{absorbance}$ (background corrected).

Supplementary References

- 1 Sleight, S. C., Bartley, B. A., Lieviant, J. A. & Sauro, H. M. Designing and engineering evolutionary robust genetic circuits. *J Biol Eng* **4**, 12, (2010).
- 2 Pedelacq, J. D., Cabantous, S., Tran, T., Terwilliger, T. C. & Waldo, G. S. Engineering and characterization of a superfolder green fluorescent protein. *Nat Biotechnol* **24**, 79-88, (2006).
- 3 Andersen, J. B. *et al.* New unstable variants of green fluorescent protein for studies of transient gene expression in bacteria. *Appl Environ Microbiol* **64**, 2240-2246, (1998).
- 4 Gonzalez, M., Frank, E. G., Levine, A. S. & Woodgate, R. Lon-mediated proteolysis of the Escherichia coli UmuD mutagenesis protein: in vitro degradation and identification of residues required for proteolysis. *Genes Dev* **12**, 3889-3899, (1998).
- 5 Shis, D. L. & Bennett, M. R. Library of synthetic transcriptional AND gates built with split T7 RNA polymerase mutants. *Proc Natl Acad Sci U S A* **110**, 5028-5033, (2013).
- 6 Spronk, C. A. *et al.* Hinge-helix formation and DNA bending in various lac repressor-operator complexes. *EMBO J* **18**, 6472-6480, (1999).
- 7 Shin, I., Kim, J., Cantor, C. R. & Kang, C. Effects of saturation mutagenesis of the phage SP6 promoter on transcription activity, presented by activity logos. *Proc Natl Acad Sci U S A* **97**, 3890-3895, (2000).
- 8 Cotterell, J. & Sharpe, J. An atlas of gene regulatory networks reveals multiple three-gene mechanisms for interpreting morphogen gradients. *Mol Syst Biol* **6**, 425, (2010).
- 9 Munteanu, A., Cotterell, J., Sole, R. V. & Sharpe, J. Design principles of stripe-forming motifs: the role of positive feedback. *Sci Rep* **4**, 5003, (2014).
- 10 Brun, R. & Rademakers, F. ROOT - An object oriented data analysis framework. *Nucl Instrum Meth A* **389**, 81-86, (1997).
- 11 Bintu, L. *et al.* Transcriptional regulation by the numbers: applications. *Curr Opin Genet Dev* **15**, 125-135, (2005).
- 12 Bintu, L. *et al.* Transcriptional regulation by the numbers: models. *Curr Opin Genet Dev* **15**, 116-124, (2005).
- 13 McAdams, H. H. & Arkin, A. Simulation of prokaryotic genetic circuits. *Annu Rev Biophys Biomol Struct* **27**, 199-224, (1998).
- 14 Greber, D. & Fussenegger, M. An engineered mammalian band-pass network. *Nucleic Acids Res* **38**, e174, (2010).
- 15 Buchler, N. E. & Cross, F. R. Protein sequestration generates a flexible ultrasensitive response in a genetic network. *Mol Syst Biol* **5**, 272, (2009).
- 16 Moran, U., Phillips, R. & Milo, R. SnapShot: key numbers in biology. *Cell* **141**, 1262-1262 e1261, (2010).
- 17 Imburgio, D., Rong, M., Ma, K. & McAllister, W. T. Studies of promoter recognition and start site selection by T7 RNA polymerase using a comprehensive collection of promoter variants. *Biochemistry* **39**, 10419-10430, (2000).
- 18 Sambrook, J., Fritsch, E. F. & Maniatis, T. *Molecular Cloning: A Laboratory Manual*. (Cold Spring Harbor Laboratory Press 1989).
- 19 Guzman, L. M., Belin, D., Carson, M. J. & Beckwith, J. Tight regulation, modulation, and high-level expression by vectors containing the arabinose PBAD promoter. *J Bacteriol* **177**, 4121-4130, (1995).
- 20 Hansson, M. D., Rzeznicka, K., Rosenback, M., Hansson, M. & Sirijovski, N. PCR-mediated deletion of plasmid DNA. *Anal Biochem* **375**, 373-375, (2008).

- 21 Temme, K., Hill, R., Segall-Shapiro, T. H., Moser, F. & Voigt, C. A. Modular control of multiple pathways using engineered orthogonal T7 polymerases. *Nucleic Acids Res* **40**, 8773-8781, (2012).
- 22 Khlebnikov, A., Datsenko, K. A., Skaug, T., Wanner, B. L. & Keasling, J. D. Homogeneous expression of the P(BAD) promoter in Escherichia coli by constitutive expression of the low-affinity high-capacity AraE transporter. *Microbiology* **147**, 3241-3247, (2001).
- 23 Kogenaru, M. & Tans, S. J. An improved Escherichia coli strain to host gene regulatory networks involving both the AraC and LacI inducible transcription factors. *J Biol Eng* **8**, 2, (2014).
- 24 Baba, T. *et al.* Construction of Escherichia coli K-12 in-frame, single-gene knockout mutants: the Keio collection. *Mol Syst Biol* **2**, 2006 0008, (2006).
- 25 Sohka, T. *et al.* An externally tunable bacterial band-pass filter. *Proc Natl Acad Sci U S A* **106**, 10135-10140, (2009).
- 26 Basu, S., Gerchman, Y., Collins, C. H., Arnold, F. H. & Weiss, R. A synthetic multicellular system for programmed pattern formation. *Nature* **434**, 1130-1134, (2005).
- 27 Untergasser, A. *et al.* Primer3Plus, an enhanced web interface to Primer3. *Nucleic Acids Res* **35**, W71-74, (2007).
- 28 Kanno, J. *et al.* "Per cell" normalization method for mRNA measurement by quantitative PCR and microarrays. *BMC Genomics* **7**, 64, (2006).